M.Tech (Power Electronics and Systems)

Kumar Gaurav

2024

MODELLING AND CONTROL OF HALF BRIDGE AND NOVEL SIDO BOOST/BUCK DC-DC CONVERTER SYSTEMS

A DISSERTATION

SUBMITTED IN PARTIAL FULFILLMENT OF THE REQUIREMENTS

FOR THE AWARD OF THE DEGREE

OF

MASTER OF TECHNOLOGY

IN

POWER ELECTRONICS AND SYSTEMS

Submitted by:

KUMAR GAURAV

2K22/PES/08

Under the supervision of

PROF. DHEERAJ JOSHI

(Professor, EED, DTU)

MR. SHREYANSH UPADHYAYA

(Assistant Professor, EED, DTU)

DEPARTMENT OF ELECTRICAL ENGINEERING

DELHI TECHNOLOGICAL UNIVERSITY

(Formerly Delhi College of Engineering)

Bawana Road, Delhi-110042

JUNE, 2024

DEPARTMENT OF ELECTRICAL ENGINEERING
DELHI TECHNOLOGICAL UNIVERSITY
(Formerly Delhi College of Engineering)
Bawana Road Delhi-110042

DECLARATION

I, KUMAR GAURAV, Roll No. 2K22/PES/08 student of M.Tech (Power Electronics and Systems), hereby declare that the project Dissertation titled **"Modelling and Control of Half-Bridge and Novel SIDO Boost/Buck DC-DC Converter Systems"** which is submitted by me to the Department of Electrical Engineering Department, Delhi Technological University, Delhi in partial fulfilment of the requirement for the award of the degree of Master of Technology, is original work and not previously used for the award of any Degree.

Place: Delhi

KUMAR GAURAV

Date: 7th June 2024

DEPARTMENT OF ELECTRICAL ENGINEERING
DELHI TECHNOLOGICAL UNIVERSITY
(Formerly Delhi College of Engineering)
Bawana Road, Delhi-110042

CERTIFICATE

This is to certify that the dissertation **"Modelling and Control of Half-Bridge and Novel SIDO Boost/Buck DC-DC Converter Systems"** being submitted by KUMAR GAURAV (2K22/PES/08) in partial fulfillment of the requirements for the award of Master of Technology degree in "ELECTRICAL ENGINEERING" with specialization of "POWER ELECTRONICS & SYSTEMS" at the Delhi Technological University is an authentic work carried out by him under my supervision and guidance. To the best of my knowledge, the matter embodied in the thesis has not been submitted to any other University/ Institute for the award of any degree or diploma.

Prof. DHEERAJ JOSHI
SUPERVISOR
Electrical Engineering Department
Delhi Technological University

Mr. SHREYANSH UPADHYAYA
CO-SUPERVISOR
Electrical Engineering Department
Delhi Technological University

ACKNOWLEDGEMENT

It is a matter of great pleasure for me to present my dissertation report on "**Modelling and Control of Half-Bridge and Novel SIDO Boost/Buck DC-DC Converter Systems**." First and foremost, I am profoundly grateful to my supervisors, Prof. Dheeraj Joshi and Mr. Shreyansh Upadhyaya, from the Department of Electrical Engineering, for their expert guidance and continuous encouragement throughout all stages of my thesis. Their valuable information and timely provision of research papers brought this thesis to life. I feel fortunate to have had the opportunity to work with them. Understanding the subject deeply and interpreting the results from the graphs was a thought-provoking experience, and their kindness and generosity helped me morally complete the project even before starting it.

I would also like to extend my heartfelt thanks to Ph.D. scholar **Mr. Ashutosh Gupta** for his unwavering support during both the best and worst moments of this journey. His presence and assistance have been invaluable.

A special thank you goes to **my parents** for their constant support, encouragement, and prayers throughout this duration. I dedicate my work to them.

Lastly, I would like to thank my peers for their camaraderie and support. Their assistance and encouragement have been crucial in successfully completing this project.

Thank you all.

Date: 7th june 2024

Place: DELHI KUMAR GAURAV

ABSTRACT

The rapid advancement in power electronics has driven a significant demand for efficient, reliable, and precise regulation methods in DC-DC converters. This thesis addresses this demand by focusing on two distinct yet complementary areas of DC-DC converter technology: the half-bridge DC-DC buck converter and the single input dual output (SIDO) step-up and step-down voltage converter. The first part of this study explores the closed-loop voltage mode regulation of a half-bridge DC-DC buck converter. This converter is renowned for its exceptional load regulation abilities, achieved through a comprehensive control strategy that ensures precise and reliable voltage regulation at the output. The approach involves deriving a mathematical model, employing state-space averaging and linearization methods, and assessing the open-loop bode plot with various input voltage dividing capacitors. This detailed analysis highlights the superiority of closed-loop voltage mode control in maintaining target output voltage amidst load changes and disturbances. Notably, the proposed controller demonstrates stable output voltage with improved transient response and decreased steady-state error compared to open-loop control. The second part of this thesis delves into the SIDO step-up and step-down voltage converter, emphasizing optimal voltage gain and the challenges posed by load and line variations. A detailed mathematical model of the SIDO converter is developed to elucidate its behavior under diverse operating conditions. The study places particular importance on voltage gain characteristics and the converter's performance in varying load and line scenarios. To enhance control and stability, a Proportional-Integral (PI) controller is designed and optimized using MATLAB, ensuring efficient regulation of output voltages. Experimental validation underscores the control strategy's effectiveness, showcasing enhanced voltage regulation, reduced output voltage ripples, and improved transient response. By integrating small signal modelling, voltage mode control, and the PI controller methodology, this research offers significant contributions to the fields of half-bridge buck converters and SIDO converters. The findings presented herein advance the understanding and application of these converters in power electronics, providing valuable insights for efficient power conversion in various system.

TABLE OF CONTENTS

LIST OF ABBREVIATION

HBBC	Half -bridge buck converter
VCM	Voltage mode control
PI	Proportional integral
CCM	Continuous conduction mode
SIDO	Single input double output
SIMO	Single input multiple output
PWM	Pulse width modulation

LIST OF FIGURES

CHAPTER 1
INTRODUCTION

1.1 BACKGROUND

Within the broad field of power electronics, the growing need for advanced, dependable, and exact voltage control techniques emphasizes the important part DC-DC converters perform in many different contemporary technological environments. From portable electronics to renewable energy systems, where they must satisfy strict performance criteria defined by modern technology, these converters are essential in many different applications. With an emphasis on two major types of converters—the half-bridge DC-DC buck converter, which is adept at step-down voltage applications, and the single input dual output (SIDO) voltage converter, capable of both stepping up and stepping down voltages depending on system requirements—the thrust of this thesis is to investigate advanced control strategies for voltage control.

1.1.1 HALF-BRIDGE DC-DC BUCK CONVERTER

The discussion starts with the half-bridge DC-DC buck converter, well-known for its high efficiency and simple design. Accurate voltage regulation in such converters is crucial for consistently maintaining the desired output voltage, even when there are fluctuations in load and input voltage. This requirement demands advanced control strategies. This thesis takes a thorough approach, beginning with the development of a mathematical model using state-space averaging and linearization techniques. These methods are essential for simplifying the complex dynamics encountered in these converters, making the analysis and design of control strategies more manageable. Examining the open loop bode plot with different input voltage dividing capacitors provides important insights into the frequency response and stability of converters. This is crucial for developing effective control mechanisms. The focus is on closed-loop voltage mode control, which is well-known for its ability to effectively regulate load. This method guarantees the attainment of consistent and dependable operation by effectively maintaining the desired output voltage, even in the face of disruptions and fluctuations in load. In practical scenarios, closed-loop systems exhibit superior

transient response and reduced steady-state error when compared to open-loop control, highlighting their effectiveness.

1.1.2 SINGLE INPUT DUAL OUTPUT (SIDO) VOLTAGE CONVERTER

The versatility of the Single Input multiple Outlet (SIDO) converter in offering multiple voltage conversion possibilities from a single input source is explained. This adaptability is especially advantageous in applications that necessitate the use of numerous output voltages. Nevertheless, the task of effectively handling the inherent complexities of attaining the most favourable voltage amplification while simultaneously dealing with fluctuations in load and line conditions poses substantial difficulties. A comprehensive mathematical model of the SIDO converter is created to examine its behaviour under different operating conditions. This model offers a comprehensive understanding of the voltage gain properties and the converter's response to dynamic variations in load and input voltage. The study focuses on the installation of a Proportional-Integral (PI) controller and highlights its design and optimization using MATLAB. The goal is to improve the stability and response of the converter. The PI controller's ability to effectively manage steady-state faults and improve system dynamics is emphasized. The adjustment of the controller's parameters is thorough, with the goal of efficiently regulating the output voltages to provide stable operations under various conditions. The experimental validation of the proposed control strategy demonstrates substantial enhancements in voltage regulation, decreased output voltage ripples, and improved transient response. This highlights the practical advantages and operating efficiency that may be achieved using the recommended control method.

This thesis aims to make a valuable contribution to the field of power electronics by presenting detailed analyses and enhancement strategies for both the half-bridge DC-DC buck converter and the SIDO voltage converter. This research demonstrates the significant impact that well-planned and executed control strategies can have on enhancing the efficiency and dependability of crucial components in contemporary electronic and electrical systems.

1.2 LITERATURE REVIEW

Half-bridge DC-DC buck converters and single-input double-output (SIDO) boost converters play a crucial role in power electronics, serving current energy-efficient systems that require small size, great reliability, and outstanding performance. As a result, there has been a significant increase in research efforts in the literature to improve the design, control, and application strategies of these converters.

Half-bridge DC-DC buck converters are commonly employed in applications that demand effective step-down voltage regulation and high-power density. The half-bridge topology divides the input voltage, hence decreasing the voltage strain on the switching components. By optimizing this process, it has become possible to utilize MOSFETs with lower voltage ratings and lower on-resistance, resulting in enhanced efficiency. Recent developments have mostly concentrated on minimizing the losses that occur during switching, frequently utilizing Zero Voltage Switching (ZVS) methods. Studies [30] have further developed the incorporation of innovative soft-switching approaches that decrease the complexity of circuits, resulting in improved efficiency and reduced electromagnetic interference (EMI) emissions across a wide range of loads. Another main focus has been adaptive control techniques [29]-[31].an intelligent controller dynamically changing the switching frequency and duty cycle in response to load fluctuations. This adjusts the converter's reaction for best efficiency over several running settings. Furthermore, the discussion is efficiency enhancement by means of material advances. Researchers like yan Deng (2009) have argued for the use of Gallium Nitride (GaN) since it provides better switching frequencies and less losses than conventional Silicon-based equivalents.

On the other hand, SIDO boost converters play a crucial role in systems that require multiple output voltages while still being compact in size. This topology is particularly important in battery-powered applications where maximizing runtime without sacrificing performance is essential. The SIDO boost converter's ability to provide two different output voltages from a single input has sparked interest in the development of multi-loop control systems that can maintain the stability and regulation of both outputs separately [32]-[35]

On the other hand, SIDO boost converters play a crucial role in systems that require multiple output voltages while still being compact in size. This topology is particularly important in battery-powered applications where maximizing runtime without sacrificing performance is essential. The SIDO boost converter's ability to provide two different output voltages from a single input has sparked interest in the development of multi-loop control systems that can maintain the stability and regulation of both outputs separately [22]-[23]

The trajectory of both converter types indicates a move towards more advanced and interconnected systems. Research conducted by Koritala et al. (2022) highlighted the importance of integrating digital control systems that are programmable, flexible, and equipped with advanced algorithms like artificial intelligence and machine learning. These systems can automatically predict and adjust to meet the demands of the system. The incorporation of both converters in renewable energy systems, especially solar and wind, has been a hub of innovation. Here, the focus is on optimizing energy extraction, improving conversion efficiency, and providing reliable power to the grid or loads.p. patra (2013) research showcase the growing trend of combining buck and boost functionalities in hybrid converter systems, which effectively address complex energy scenarios [36]-[38].

To summarize, the ever-changing field of study regarding half-bridge DC-DC buck converters and SIDO boost converters indicates a continuous effort to improve efficiency in line with the changing energy industry. The constant progress in switch technologies, control techniques, and integration approaches highlights the crucial importance of these converters in various applications, including consumer electronics, industrial power systems, and renewable energy platforms. It is crucial to keep up with the expanding literature in order to properly comprehend and apply cutting-edge converter technologies.

1.3 THESIS ORGANIZATION AND CONTRIBUTION

This thesis is organized into several chapters, each focusing on different aspects of the study on half-bridge DC-DC buck converters and single input dual output (SIDO) boost/buck DC-DC converters. The structure is designed to provide a comprehensive understanding of the methodologies, analysis, and findings of the research. The thesis

organization is as follows:

Chapter-1 Provides an overview of the importance of efficient, reliable, and precise regulation methods in DC-DC converters. It outlines the growing demand in the field of power electronics and introduces the primary objectives of the study, focusing on half-bridge DC-DC buck converters and SIDO converters. A detailed literature review is presented, summarizing existing research on DC-DC converters. The review covers control strategies, mathematical modelling techniques, and the challenges faced in maintaining voltage stability and gain. It highlights the gaps in current knowledge that this thesis aims to address.

Chapter-2 Details the derivation of a mathematical model for the half-bridge buck converter. It explains the use of state-space averaging and linearization methods to simplify the model. The chapter also includes an assessment of the open-loop Bode plot for various input voltages and capacitors, providing insights into the frequency response and stability of the system.

Chapter-3 Details the implementation of control methodologies for the half-bridge buck a, presenting MATLAB simulation results. It discusses the effectiveness of the closed-loop and PI control strategies, highlighting improvements in voltage regulation, transient response, and output stability under various conditions.

Chapter-4 Presents the design and mathematical modeling of the novel SIDO boost/buck DC-DC converter. It explores the converter's dual output capabilities, behavior under varying conditions, and optimization of voltage gain, setting the foundation for enhanced control and stability strategies.

Chapter-5 Details the implementation of control methodologies for The IDO converter, presenting MATLAB simulation results. It discusses the effectiveness of the closed-loop and PI control strategies, highlighting improvements in voltage gain, transient response, and output stability under various conditions.

Chapter-6 Concludes with a summary of the key findings and contributions of the research. It outlines the advancements made in voltage stability and gain enhancement for DC-DC converters. The chapter also proposes directions for future work to further improve and innovate in this field.

1.4 CONCLUSIONS

This thesis has thoroughly addressed the fundamental elements of design, analysis, and control in the context of half-bridge DC-DC buck converters and single input dual output (SIDO) boost/buck converters. Through a systematic arrangement of research material in its chapters, this work has highlighted the crucial importance of effectiveness, reliability, and accuracy in the field of DC-DC conversion. This represents a significant advancement in the area of power electronics.

The investigation of developments in control techniques for DC-DC converters, especially within the scopes of half-bridge buck and SIDO converters, forms the central focus of this work. These advances in power electronics mark a turning point by bringing in and verifying strong control systems. Such improvements satisfy the growing needs of many different applications in addition to guaranteeing effective, consistent, and exact voltage control. This opens the path for further studies aiming at exploring innovative control strategies and improving current models, so enhancing the performance and adaptability of these fundamental components in power electronics systems.

The consequences of this study go well beyond its present conclusions. This thesis offers a strong basis for next developments by clarifying the intricate behaviors of converters and their control by use of advanced control strategies. It is a great tool for next developments in the subject since it fills in a major gap in the current knowledge base. The insights and techniques presented in this work are likely to be very important in determining the design and deployment of more dependable, efficient power converters as the terrain of power electronics keeps changing and growing. This guarantees that the contributions of this thesis will be relevant far into the future, guiding next power electronics development.

CHAPTER 2
DESIGIN AND MODELLING OF ISOLATED HALF BRIDGE DC-DC CONVERTER.

This chapter provides a comprehensive introduction to the design and modelling of isolated half-bridge DC-DC converters. It covers the fundamental principles of operation, highlights the key components involved, and outlines the essential steps in the design process. Additionally, it introduces the mathematical modelling techniques necessary for analyzing and optimizing the converter performance.

2.1 INTRODUCTION

In today's technology-driven society, there is a crucial need to design power conversion systems that are efficient. This is because the demand for power sources that are both safe and reliable is of utmost importance. Isolated DC-DC converters are increasingly sought after in numerous applications, particularly those involving sensitive electronic equipment and requiring electrical separation for safety purposes. Isolated converters provide the additional benefit of electrical isolation between the input and output, which is essential for preventing ground loops, guaranteeing user safety, and maintaining compatibility with various power sources.

There are many topologies for isolated converters, each with special advantages catered for particular uses. Flyback converters, forward converters, push-pull converters, full-bridge and half-bridge isolated converters all show on the roster. Among these, the isolated half-bridge DC-DC converter has become somewhat well-known. Its simplicity of circuit design—which results in manufacturing and operational cost savings while preserving good power density and efficiency—helps to explain its dominance in the scene of power electronics.

Part of the advantage of the isolated half-bridge converter is its topology, which calls for less components than the full-bridge equivalent, therefore lowering complexity and possible sites of error. Because of the fewer switches, which in turn lowers the switching losses – a major factor for any power conversion system – the architecture also offers improved efficiency. Moreover, the use of a transformer in this topology offers galvanic isolation, a necessary property in many medical and industrial uses.

Effective handling of high input voltages is another important feature of the half-bridge converter that makes it appealing. In sectors where devices must run consistently over a wide spectrum of input conditions, this is an absolutely vital trait. Furthermore, the half-bridge topology's intrinsic redundancy gives another degree of defense against system failures, hence strengthening the design [1]-[2].

But exact modelling of the operating behaviour of the isolated half-bridge DC-DC converter is very essential to fully utilize its possibilities. Achieving best performance depends on a thorough knowledge of the converter dynamics, which is made possible by accurate modeling. It is the basis upon which performance improvements, design concerns, and converter dependability and efficacy stand [3]-[4].

Modeling is essential for a variety of reasons. It helps predict how a system will respond to different inputs and loads, aids in selecting the right components to avoid saturation and other non-linear behaviors, and is vital for developing effective control strategies for the converter system. Without a strong and comprehensive model, it is difficult to determine the necessary criteria for stability, responsiveness, and efficiency, which are crucial standards for any power converter.[5]-[7].

In this particular situation, the thesis acknowledges that a widely accepted and well-established method for modeling such converters is by utilizing state-space averaging approaches. This approach is notable for its capacity to depict the dynamics of the system in a more controllable manner, taking into consideration the impacts of changing operating circumstances and non-linear behaviors [7]-[9]. State-space averaging simplifies the intricate time-domain behaviors of the converter into an average model, enabling a more comprehensible analysis of both steady-state and transient situations. This is crucial in the development of dependable converters.

The thesis utilizes the state space averaging technique to describe the isolated half-bridge converter and generates a transfer function that reflects the system's performance. The transfer function represents the fundamental dynamics and hence, acts as a preliminary step in designing an efficient controller. The design of the controller is essential as it ensures that the converter maintains its target voltage output accurately, independent of variations in load or input conditions [9]-[10].

An advanced controller, based on a robust mathematical model, guarantees the stability of the system and improves its transient response. This is crucial for ensuring consistent operation of the converter. By originating from a legitimate model, the controller may promptly reduce disturbances, maintain voltages within specified limits, and enhance the overall resilience of the power system

To summarize, the isolated half-bridge DC-DC converter offers several appealing benefits, such as high efficiency, simplicity, and reliability, which make it a compelling choice for widespread use. Precisely simulating this converter is an essential stage in order to effectively utilize and enhance its functionalities. This thesis aims to analyze the complexities of the isolated half-bridge converter using state-space averaging. It seeks to develop a robust model that will serve as the foundation for enhanced controller design and, ultimately, a more dependable power conversion solution [11]-[12].

2.2 CIRCUIT DESCRIPTION

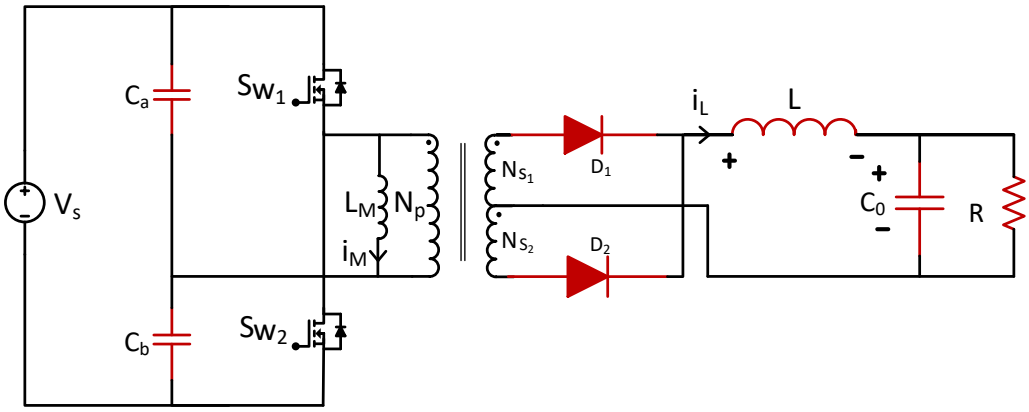

Fig 2.1 Half Bridge DC-DC Buck Converter Circuit Description

There are two main types of half-bridge isolated DC-DC converters: symmetric and asymmetric. The classification is primarily determined by the arrangement and functioning of the switches and transformer in the converter circuit. In a symmetric half-bridge converter, the two switches have equal duty cycles, which means they are activated and deactivated for the same duration during each switching cycle. The symmetry of the transformer guarantees that the average voltage across its primary side is zero for one complete cycle of switching, which helps maintain balanced

functioning. Conversely, the asymmetric half-bridge converter employs switches with varying duty cycles. This modification enables a wider spectrum of output voltage regulation, but it also brings intricacy in control and a possibility of unbalanced transformer operation.

A third-order isolated half-bridge DC-DC buck converter is composed of two switches, Sw_1 and Sw_2, two input capacitors, C_a and C_b, one output capacitor C_o and a transformer and inductor for energy transfer as shown in Fig.1.

The analysis of the converter modelling is based on the following assumptions. In steady state condition output voltage and current are constant. The transformer's leakage inductance L and the parasitic capacitance Co of switches can be considered insignificant. The duration of the inactive period between the two switch transitions is significantly smaller in comparison to the switching time period and can be neglected. The components L_m, L, and C_o does not have any series resistance. All components within the circuit show no losses, meaning that there is no voltage drop across MOSFETs, diodes, inductors, or capacitors.

2.3 MODES OF OPERATION

2.3.1 MODE 1 OF OPERATION:

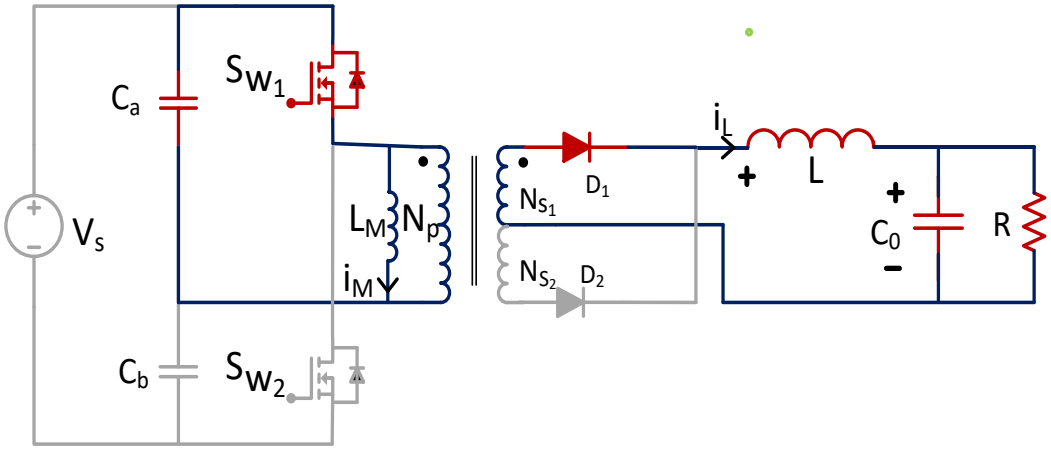

Fig2.2 Circuit Diagram when Switch (Sw_1) is close and Switch (Sw_2) is open

During the positive half cycle, the upper switch (Sw_1) is turned on, the lower switch (Sw_2) is off, allowing current to flow through the positive half of the input DC source, charging the load inductor and delivering power to the output as shown in fig.2.2

2.3.2 MODE 2 OF OPERATION

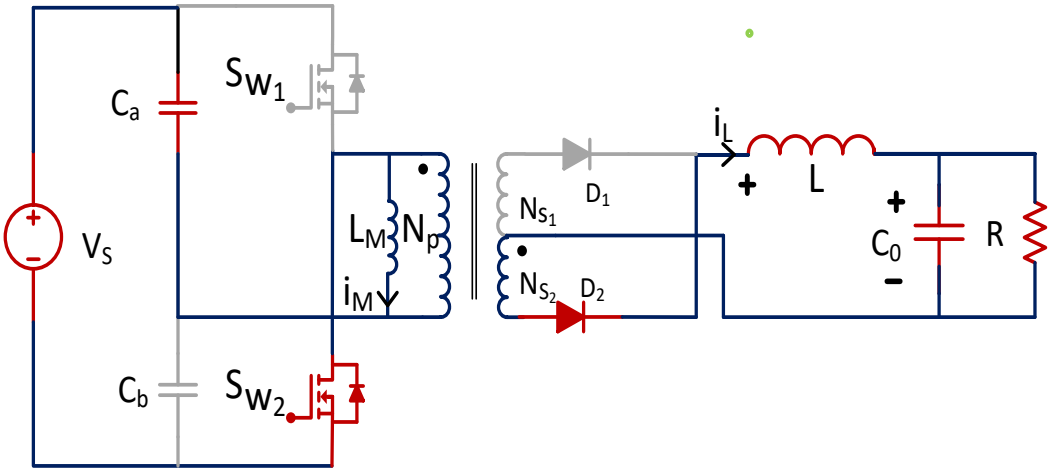

Fig 2.3 Circuit Diagram when Switch (Sw_1) is open and Switch (Sw_2) is close

Conversely, during the negative half cycle, the lower switch (Sw_2) turns on, and the upper switch (Sw_1) turns off, transferring the power stored in the inductor to the load and ensuring continuous power flow to the output.

2.3 SMALL SIGNAL ANALYSIS

Small signal analysis is a technique in electrical engineering utilized to evaluate the performance of nonlinear circuits when subjected to minor perturbations around a defined operating point. By assuming the perturbations are small enough, the nonlinear elements of the circuit can be approximated by linear models, simplifying the analysis. This involves identifying a steady-state operating point and then linearizing the circuit's components around this point. The resulting linearized circuit allows for the application of linear circuit analysis methods to determine the circuit's response to small signals, providing insights into parameters such as gain, input and output impedance, and frequency response. This method is particularly valuable for the design and analysis of DC-DC converters, analog circuits, including amplifiers and oscillators.

2.4 STEPS FOR SMALL SIGNAL MODELLING

Step 1: Identify the operating point.

To begin, it is essential to determine the state variables of the converter. Typically, the variables to consider for a DC-DC converter are the current flowing through the inductor(s) and the voltage across the capacitor(s). The selection of state variables is essential in effectively depicting the dynamics of the system.

Step 2: Model the Converter in Each Switching State

Due to the alternating on and off states of the switches in the converter, the converter can be in two distinct states during a single switching cycle. It is necessary to create a circuit model for each state.

ON State Model: In the on state, the switch allows current to flow via the inductor, transformer, and load. Additionally, voltage is applied across the capacitors.

OFF State Model: This model represents the state of the switch when it is turned off and not conducting electricity. It illustrates the flow of current through diodes or other freewheeling routes, as well as the voltage across different components.

Step 3: Formulate state equations for each state

Obtain the differential equations that describe the behavior of the state variables in both the ON and OFF states. The equations are derived from Kirchhoff's Voltage Law (KVL) and Kirchhoff's Current Law (KCL).

Step 4: Utilize the Averaging Principle

Utilize the duty cycle (D) of the switch to calculate the average of the state equations. The duty cycle denotes the ratio of the time during which the switch is in the ON state to the total switching duration. The averaged state equations are a combination of the state equations from both the ON and OFF states, with weights determined by the duty cycle and its complement (1-D), respectively.

Step 5: Obtain the Averaged State-Space Model

Formulate the averaged state-space model by consolidating the averaged state equations into a matrix representation. This model comprises a collection of linear differential equations that depict the converter's behavior across a single switching period, thereby mitigating the abrupt changes induced by switching.

Step 6: Convert the State-Space Model into a Linear Form

Linearize the averaged state-space model around an operating point if it is nonlinear. This phase is essential for simplifying the analysis and generating a transfer function that accurately captures how the system responds to tiny changes in the input signal around the operating point.

Step 7: Calculate the Transfer Function

Obtain the transfer function from the linearized averaged state-space model by applying the Laplace transform to the state equations, if needed, and solving for the ratio between the output variable and the input variable of interest. The transfer function characterizes the relationship between the input and output of the converter, providing insights into the system's dynamics and stability.

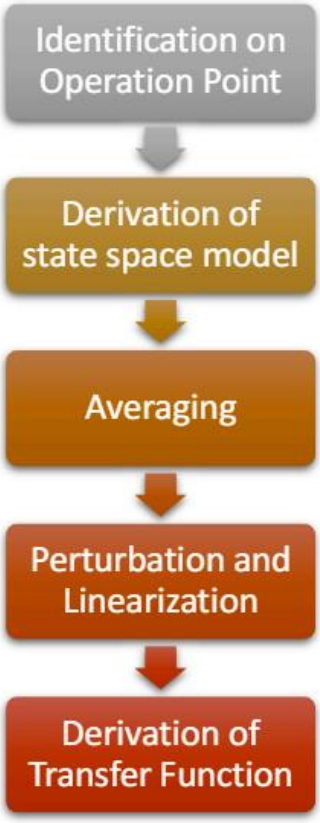

Fig 2.4 Flow chat of ac small signal modelling

A small -signal model is derived from the circuit equation to analyse circuit dynamics. The transformer magnetizing inductor current (i_M), output inductor current (i_L), input capacitor voltage (V_{C_a}) and output capacitor voltage (V_{C_o}) are state variables. Input voltage, output voltage are controlled input variable and output variable respectively of the HBBC

$$= \left[V_{C_a}\, i_M\, i_L\, V_{C_o}\right], \quad u = [V_s], \quad y = [V_o] \qquad 2.1$$

The state space representation of the system is described by the generalized set of equations:

$$\dot{x} = AX + BU$$
$$y = CX + EU \qquad 2.2$$

the state matrix is denoted by A, the input matrix is denoted by B, the output matrix is denoted by C, and the input output coupling matrix is denoted by D.

2.4 STATE SPACE EQUATION

State space equations are a mathematical representation used in control theory and systems engineering to model and analyse the dynamic behaviour of systems. This representation employs a set of first-order differential equations to describe the evolution of the system's state variables over time. The differential equations of the HBBC converter in Mode 1 are as follows:

$$\frac{dV_{C_a}}{dt} = -\frac{i_M}{2C_a} - \frac{i_L}{2N_1C_a} \tag{2.3}$$

$$\frac{di_M}{dt} = \frac{V_{C_a}}{L_M} \tag{2.4}$$

$$\frac{di_L}{dt} = \frac{V_{C_a}}{N_1L} - \frac{V_{C_o}}{L} \tag{2.5}$$

$$V_{C_o} = \frac{i_L}{C_o} - \frac{V_{C_o}}{RC_O} \tag{2.6}$$

$$\begin{aligned}\left[V_{C_a}\ i_M\ i_L\ V_{C_o}\right] &= \left[0\ -\frac{1}{2C_a}\ -\frac{1}{2N_1C_a}\ 0\ \frac{1}{L_M}\ 0\ 0\ 0\ \frac{1}{N_1L}\ 0\ 0\right. \\ &\left. -\frac{1}{L}\ 0\ 0\ \frac{1}{C_o}\ -\frac{1}{RC_O}\right]\ \left[V_{C_a}\ i_M\ i_L\ V_{C_o}\right] + [0\ 0\ 0\ 0\ ]V_s\end{aligned} \tag{2.7}$$

The differential equations of the HBBC converter in mode II are as follows:

$$\frac{dV_{C_a}}{dt} = -\frac{i_M}{2C_a} - \frac{i_L}{2N_2C_a} \tag{2.8}$$

$$\frac{di_M}{dt} = \frac{V_{C_a}}{L_M} - \frac{V_s}{L_M} \tag{2.9}$$

$$\frac{di_L}{dt} = -\frac{V_{C_a}}{N_2L} - \frac{V_{C_o}}{L} + \frac{V_s}{N_2L} \tag{2.10}$$

$$V_{C_o} = \frac{i_L}{C_o} - \frac{V_{C_o}}{RC_O} \tag{2.11}$$

$$\begin{aligned}\left[V_{C_a}\ i_M\ i_L\ V_{C_o}\right] &= \left[0\ -\frac{1}{2C_a}\ -\frac{1}{2N_2C_a}\ 0\ \frac{1}{L_M}\ 0\ 0\ 0\ -\frac{1}{N_2L}\ 0\ 0\right. \\ &\left. -\frac{1}{L}\ 0\ 0\ \frac{1}{C_o}\ -\frac{1}{RC_o}\right]\ \left[V_{C_a}\ i_M\ i_L\ V_{C_o}\right] \\ &+ \left[0\ -\frac{1}{L_M}\ \frac{1}{N_2L}\ 0\right] V_s\end{aligned} \tag{2.12}$$

The switching waveform of the circuit in both the mode of operation is shown below:

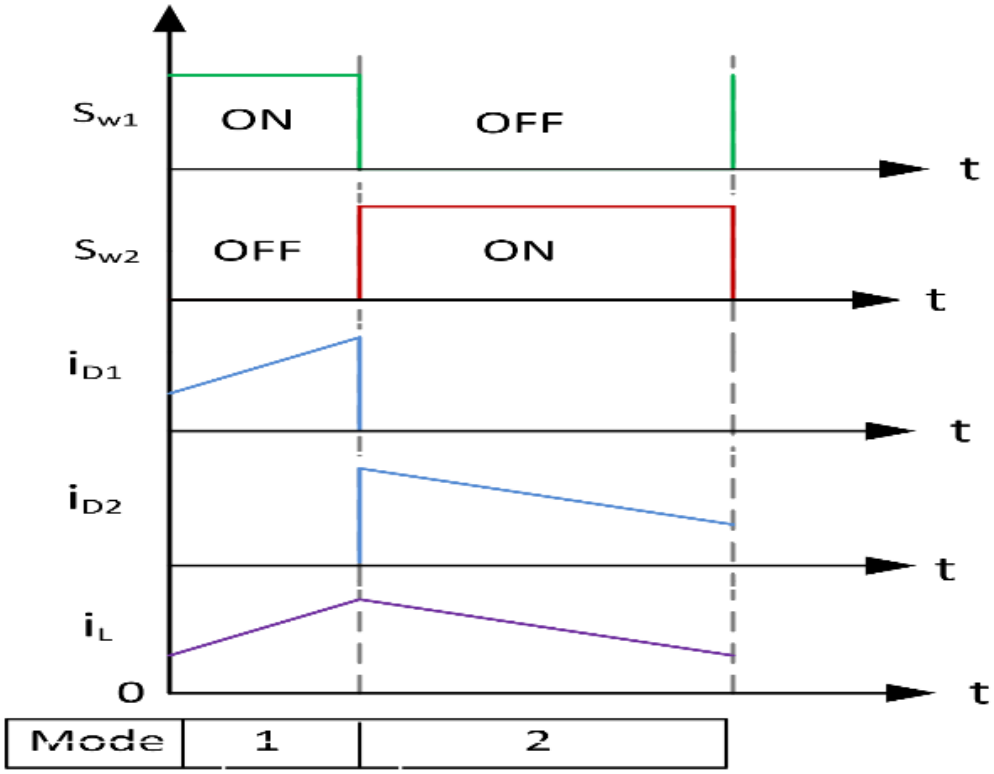

Fig.2.5 Switching waveform for switches, diodes, and inductor

Table 2.1 Design parameter of half bridge DC-DC buck converter

Parameters	Symbols	Values
Input Voltage	V_s	220 V
Output Voltage	V_o	48 V
Switching Frequency	f_{sw}	100 kHz
Duty Cycle	D	0.218
Magnetizing Inductance	L_m	500µH
Filter Inductor	L	800µH
Filter Capacitor	C_0	300µF
Load Resistance	R	24Ω
Secondary Winding 1	N_{s_2}	1
Secondary Winding 2	N_{s_1}	1
Current Ripple	ΔI_o	20% I_o
Voltage Ripple	ΔV_o	1%V_o

The switching waveforms of the diode, inductor, and switches are illustrated in Fig. 2.4 for two distinct modes, Mode 1 and Mode 2. In Mode 1, Switch 1 is in the on state while Switch 2 is in the off state. During this mode, Diode 1 is conducting, and Diode 2 is not conducting, resulting in the inductor being charged. Conversely, in Mode 2, Switch 2 transitions to the on state and Switch 1 to the off state. In this mode, the inductor discharges through Diode 2, which is now conducting, while Diode 1 is off.

To mitigate the impact of the switching ripple component on the circuit equations, a technique of averaging across a single switching period is employed. The averaged switching model is obtained by calculating the average of the aforementioned equations over a single switching period according to Fig.3.

$$A = A_1 d + A_2(1-d) \tag{2.13}$$

$$B = B_1 d + B_2(1-d) \tag{2.14}$$

$$C = C_1 d + C_2(1-d) \tag{2.15}$$

$$D = D_1 d + D_2(1-d) \tag{2.16}$$

In order to obtain the small signal model of the isolated half bridge DC-DC buck converter, it is essential to linearize the nonlinear averaged state-space model in relation to a specified operating point. The introduction of perturbations is employed to modify the state variables (i_m, i_L, V_{Ca}, V_{Co}), input variables (V_s), output variables (V_o), and duty cycle (D).

$$\begin{aligned} d &= D + \hat{d} \\ x &= X + \hat{x} \\ u &= U + \hat{u} \\ y &= Y + \hat{y} \end{aligned} \tag{2.17}$$

The linearized small signal model is obtained by incorporating the perturbed variables into the averaged state-space model Eq. while disregarding the higher order terms.

$$s\hat{x}(s) = A\hat{x}(s) + B\hat{u}(s) + ((A_1 - A_2)X(s) + (B_1 - B_2)U(s))\hat{d}(s) \tag{2.18}$$

$$\hat{y}(s) = C\hat{x}(s) + D\hat{u}(s) + ((A_1 - A_2)X(s) + (D1 - D2)U(s))\hat{d}(s) \tag{2.19}$$

$$\frac{\hat{x}(s)}{\hat{d}(s)} = (sI - A)^{-1}((A_1 - A_2)X(s) + (B_1 - B_2)U(s)) \tag{2.20}$$

Using Equation, the output-to-control transfer function can be obtained by substituting the values of the parameters from Table I.

$$\frac{\hat{V_o}(s)}{\hat{d}(s)} = \frac{\alpha_{12}s^2 + \alpha_{11}s + \alpha_{10}}{s^4 + \beta_3 s^3 + \beta_2 s^2 + \beta_1 s + \beta_0} \tag{2.21}$$

The control to output transfer function is given by:

$$\frac{\hat{V_o}}{\hat{d}} = \frac{4.7 \times 10^8 s^2 + 4.273 \times 10^{10} s + 9.4 \times 10^{15}}{s^4 + 1.578 \times 10^7 s^3 + 1.514 \times 10^9 s + 3.788 \times 10^{13}} \tag{2.22}$$

This specific transfer function encapsulates the relationship between the converter's output voltage and the duty cycle. The transfer function of the output voltage to duty cycle is crucial for achieving accurate control over the output voltage. Ensuring a consistent and precise output voltage is crucial in real-world scenarios, irrespective of fluctuations in input voltage or alterations in the load. The transfer function facilitates the adjustment of the duty cycle to counter disturbances, allowing real-time control techniques like as Pulse Width Modulation (PWM) to effectively maintain desired voltage levels.

Furthermore, from a design standpoint, this transfer function provides engineers with crucial insights. Through the analysis of this function, it is possible to anticipate the impact of alterations in the converter's settings or operating conditions on its performance. By adjusting the duty cycle, it becomes feasible to predict the consequences, which helps in choosing suitable components and determining the best operating points that align with required performance standards. Moreover, the transfer function is of utmost importance in stability analysis. Through the analysis of the properties of this function, specifically its poles and zeros, engineers may evaluate how the system will react to disturbances and detect any possible stability problems. Conducting this proactive analysis is essential because it provides the information needed to make the necessary compensations or tweaks to the control strategy. This ensures that the converter functions reliably in all anticipated circumstances

CHAPTER 3
CONTROL METHODOLOGY

3.1 INTRODUCTION

For the isolated half bridge DC-DC buck converter to achieve the desired voltage regulation, improve dynamic response, and increased system stability, closed-loop control must be used. In this study, the proportional integral (PI) controller utilized in closed-loop half bridge DC-DC converter with voltage mode control is thoroughly studied, and its effects on the converter's overall performance is evaluated.

The closed-loop regulation of a half-bridge DC-DC buck converter is crucial for achieving accuracy in output voltages that are used in important applications. The necessity for closed-loop control arises from the fact that real-world situations often cause disruptions, such as variations in input voltage, alterations in load, and imperfections in components. If not monitored, these factors can cause substantial variations from the intended output voltage. Closed-loop control systems continuously monitor the output, compare it to the desired setpoint, and dynamically alter the control input to correct any deviations, ensuring a steady and consistent output despite external disturbances or internal variations.

In order to provide closed-loop voltage mode control in these converters, we have utilized a closed-loop Proportional-Integral (PI) controller. This controller effectively handles the system's dynamics to ensure that the desired voltage is maintained by consistently correcting any discrepancies found in the output voltage. The PI controller combines the immediate error proportionality with the integral of past errors to provide the system with both reactive and anticipatory control actions. The proportional term generates a response that is directly proportionate to the current error, whereas the integral term aims to eliminate any remaining steady-state error by integrating the error over time.

3.2 CLOSED LOOP VOLTAGE MODE CONTROL

Voltage mode control operates by directly adjusting the duty cycle of the converter in response to output voltage readings. Put simply, the control variable is the voltage, and modifications are made to the switching element in the converter to ensure that this

voltage remains at a predetermined level. The PI controller in the voltage mode control scheme perceives every deviation between the actual output voltage and the desired voltage as an error, which it methodically reduces by altering the duty cycle correspondingly as shown in the below figure:

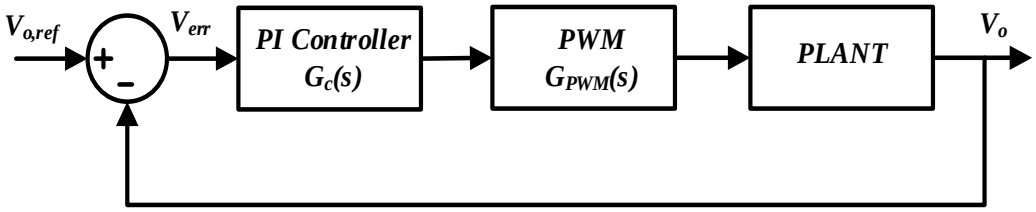

Fig. 3.1 Closed loop voltage mode control diagram

The HBBC converter, a non-linear system, is susceptible to variations in the input voltage, load current, and various external factors. Hence, the implementation of a closed-loop control system becomes imperative in order to effectively regulate the output voltage of the HBBC converter. In the absence of a closed-loop control system, it is observed that the output voltage exhibits fluctuations, thereby posing a potential risk of detrimental consequences to both the load and the converter.

The closed-loop voltage mode control technique is employed to effectively regulate the output voltage of the HBBC converter. This control method operates by dynamically adjusting the duty cycle of the converter in response to the error signal, which represents the discrepancy between the desired output voltage and the actual output voltage. By continuously monitoring and adapting the duty cycle, the closed-loop voltage mode control ensures that the HBBC converter maintains a stable and accurate output voltage as shown in fig (3.1). The closed-loop control system is widely recognized for its ability to deliver exceptional output voltage regulation and rapid transient response, rendering it highly suitable for a diverse range of applications necessitating power flow.

The transfer function of PI controller is given as:

$$G_c(s) = K_{prop} + \frac{K_{int}}{s} \tag{3.1}$$

$$G_c(s) = 1.8344 \times 10^{-2} + \frac{0.56521}{s} \tag{3.2}$$

where K_{pro}, K_{int} denote the proportional, integral, derivative gains which are selected as $K_{prop} = 1.8344 \times 10^{-2}, K_{int} = 0.56521$, which is calculated with the help of ziegler-Nichols Method.

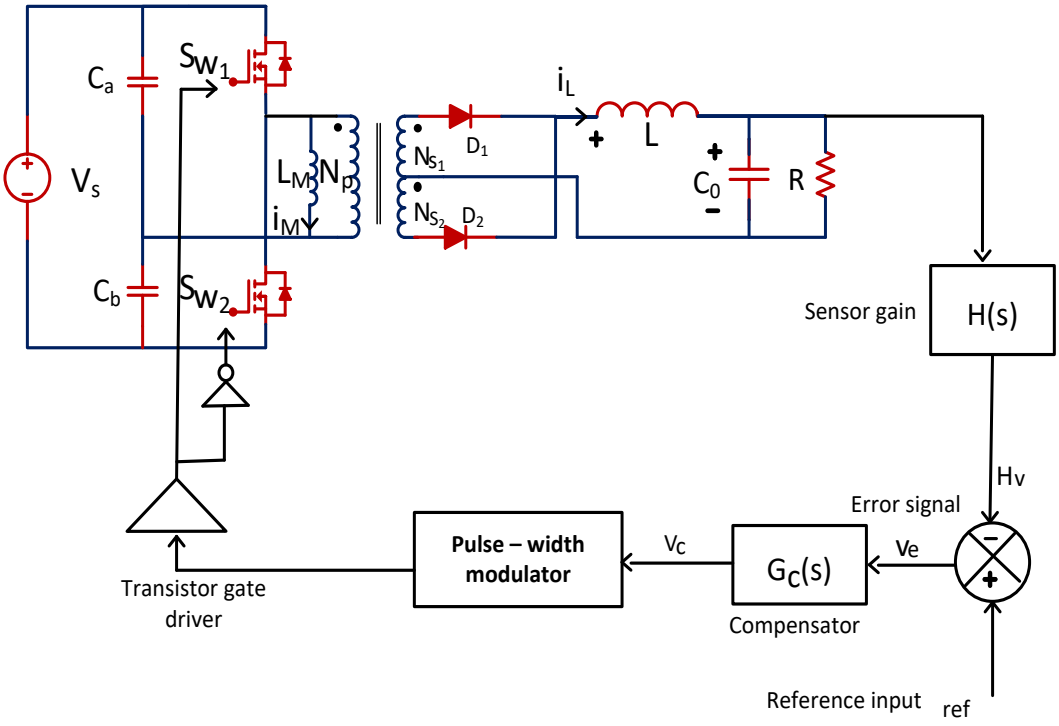

Fig 3.2 Voltage mode control loop for HBBC Converter

The small signal model for the closed loop voltage mode control system is shown in the figure.

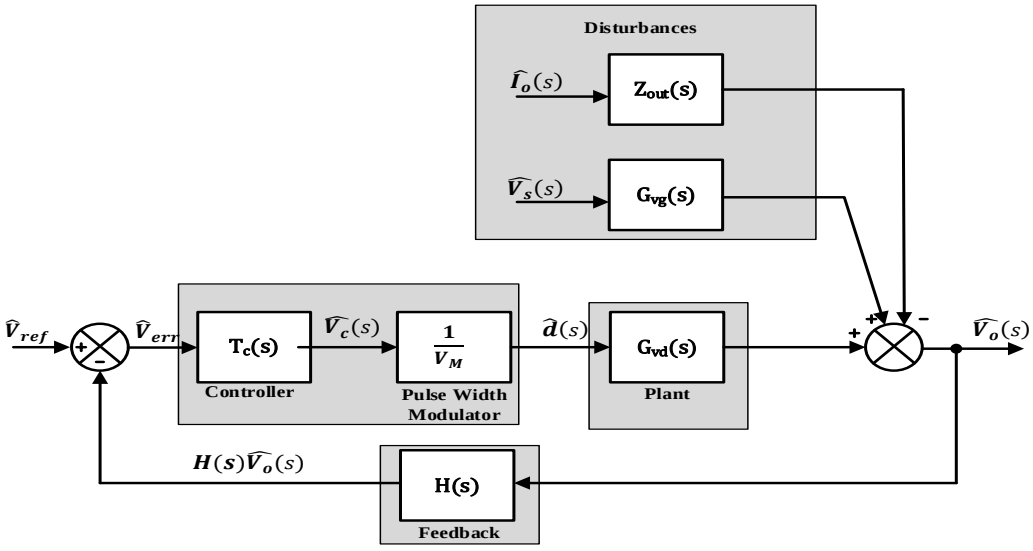

Fig 3.3 Close loop voltage mode control loop for HBBC Converter

The reference to the output closed-loop transfer function is given by:

$$\frac{\hat{V}_{ref}}{\hat{V}_o} = \frac{\alpha_{23}s^3 + \alpha_{22}s^2 + \alpha_{21}s + \alpha_{20}}{s^5 + \beta_4 s^4 + \beta_3 s^3 + \beta_2 s^2 + \beta_1 s + \beta_0} \quad (3.3)$$

Where the constant values are given as follows

$$\frac{\hat{V}_{ref}}{\hat{V}_o} = \frac{8.622 \times 10^6 s^3 + 1.049 \times 10^9 s^2 + 1.725 \times 10^{14} s + 5.313 \times 10^{15}}{s^5 + 126.3 s^4 + 2.44 \times 10^7 \ s^3 + 2.563 \times 10^9 s^2 + 2.103 \times 10^{14} s + 5.313 \times 10^{15}}$$

Fig 3.4 displays the bode plot of the open loop plant, illustrating the variations resulting from different input capacitor values, C_a. Three different capacitance values were used for C_a are 100µF, 200µF, and 330µF. The presented figure illustrates that alterations in the values of capacitors result in variations in the phase margin of the open loop system. The phase margin for a 100µF capacitor is -0.773 degrees, indicating a high level of instability in the open loop system. However, when using a 200µF capacitor, there is a slight improvement in the phase margin, which increases to 5.96 degrees. The phase margin for a capacitor with a capacitance of 330 µF is measured to be 6.54 degrees. An increase in the value of capacitor C_a leads to an enhancement in the phase margin of the open loop system. This study helps in selection of C_a capacitor value

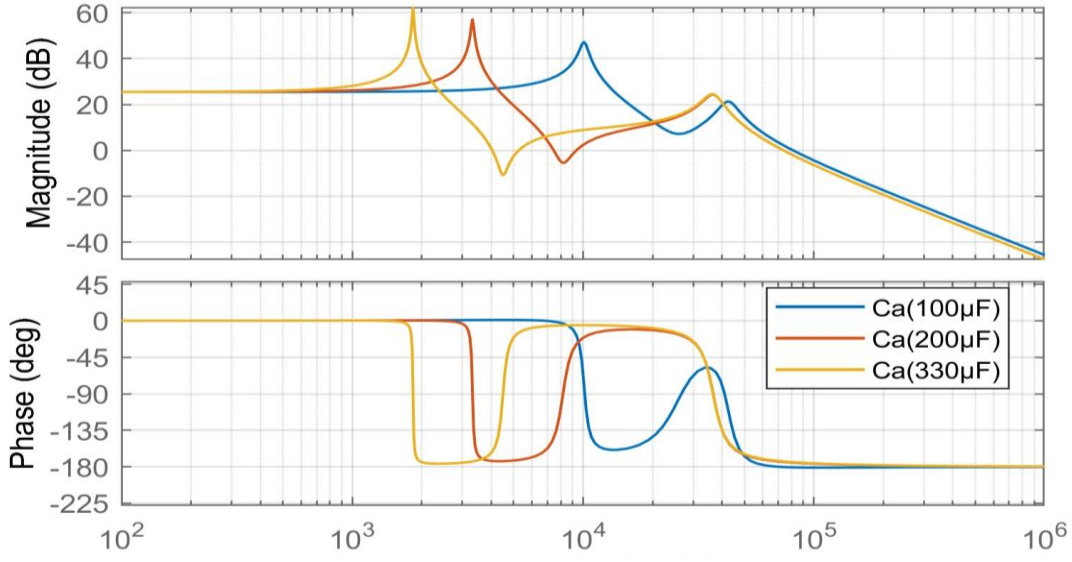

Fig. 3.4 Open loop frequency response with variation in C_a of Half bridge DC-DC buck converter

While it is true that the stability of a system increases with an increase in phase margin,

this improvement is accompanied by a trade-off in the form of a slower response time. In order to achieve optimal response time and system stability, the value of C_a is selected as 200 µF for the design of the closed-loop system.

Fig 3.5 illustrates the frequency response of the closed loop system. The closed loop system exhibits a phase margin of 78 degrees, indicating a significantly higher level of stability in comparison to its open loop counterpart.

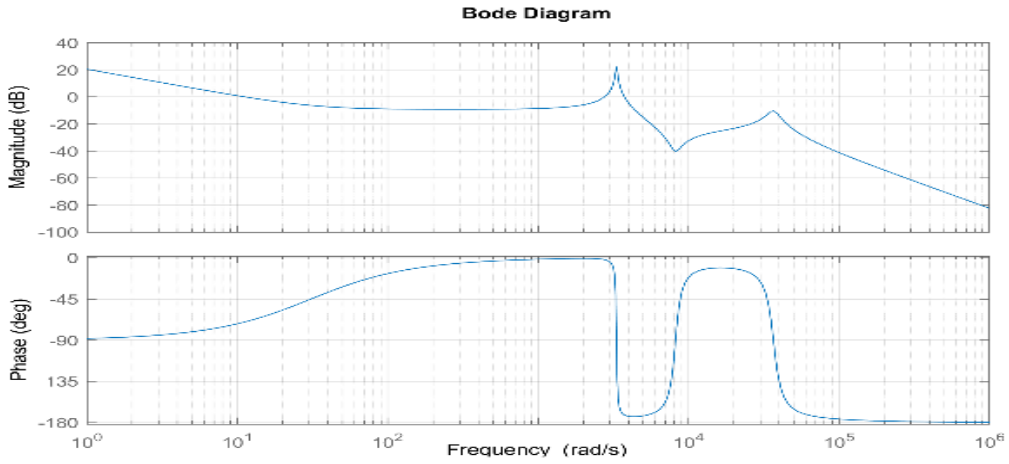

Fig 3.5 Bode plot of closed loop system of half bridge DC-DC buck converter

3.3 RESULTS AND DISCUSSION

The design and modeling of the Half bridge DC-DC buck converter in conducted using MATLAB/Simulink. Additionally, the PI controller was developed and calibrated using the Phase Margin test methodology

3.3.1 Open Loop Vs Closed Loop Voltage Comparison

Fig 3.6. depicts the output voltage characteristics of the half bridge buck converter in both open and closed loop configurations. The open loop system exhibits a maximum peak overshoot of 51%, from 48V to 72.24V whereas the closed loop system demonstrates a maximum peak overshoot of 9.85% from 48V to 53.72 V. This observation suggests a clear correlation between the phase margin and the maximum peak overshoot. Increasing the phase margin of the system results in a reduction in the peak overshoot.

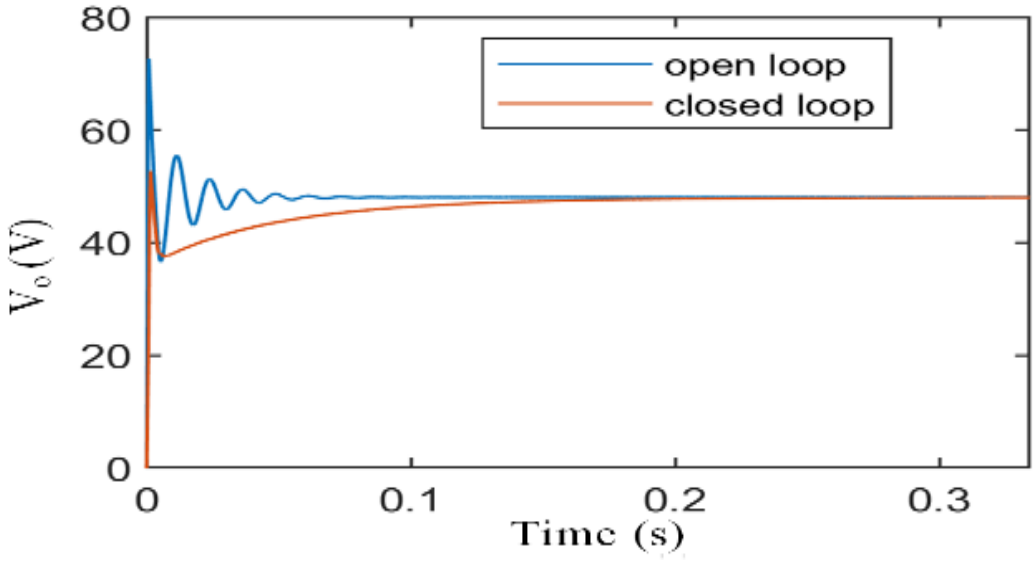

Fig 3.6 Open loop vs closed loop Half bridge DC-DC buck converter output voltage

3.3.2 Load Regulation

The evaluation of the steady load regulation performance involves a step variation of the resistive load within the range of 26Ω to 48Ω. This process is accompanied by continuous monitoring of the output voltage, as illustrated in Fig. 8. Due to load change output voltage maintain the constant voltage 48 V with load current reduced from 1.8A to 1A. The simulation findings illustrate the converter's capacity to sustain a consistent output voltage within a desired load, thereby regulating output voltage precisely.

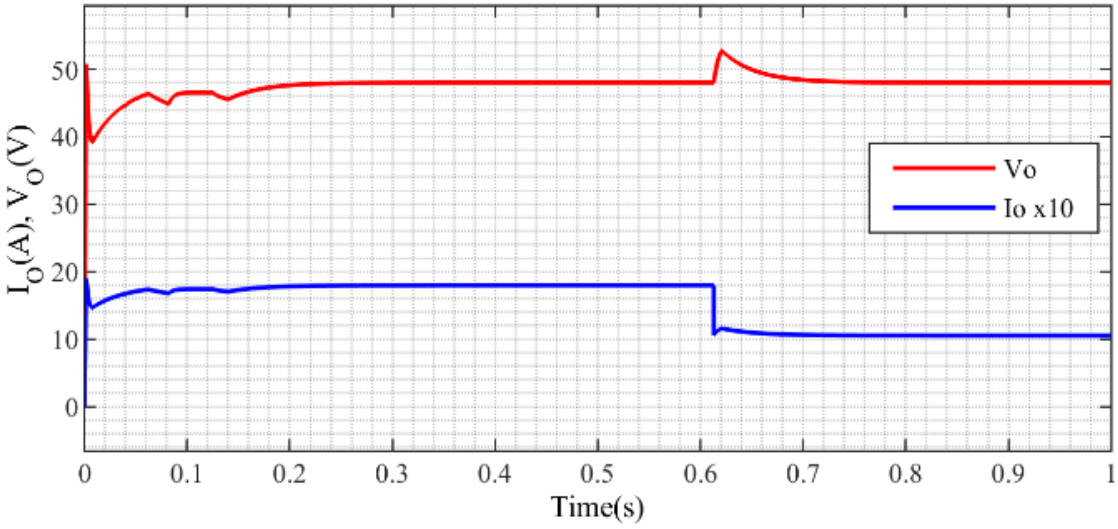

Fig.3.7 Load Regulation response of Half bridge DC-DC buck converter

3.4 CONCLUSIONS

In conclusion, this research underscores the substantial merits of employing closed-loop voltage mode control in half-bridge DC converters. Through a thorough investigation, including a small-signal analysis, we have assessed the system's stability, transient step response, and bandwidth characteristics. In the course of the investigation, the system's response to different input capacitor values is examined. This in-depth analysis proved instrumental in identifying the most suitable input capacitor with a capacitance of 200 µF, thereby enhancing the overall stability of the system, resulting a phase margin of 78 degrees. These findings both inform and propel the design, optimization, and effective application of this control strategy in numerous power electronic contexts.

Dependable output voltage of 48V is maintained via voltage mode control, even when faced with sudden load variations from 26Ω to 48Ω. It's critical to recognize, however, that achieving superior performance is fundamentally contingent upon appropriate selection of controller parameters. Additionally, the efficiency of this control approach may be modulated by different power levels or applications.

To effectively address the impact of load and line voltage variations, it is advisable to encourage further research in this domain. Subsequent investigations could center their attention on optimizing controller parameters to suit diverse operating conditions, as well as engaging in comparative analyses of alternative control strategies. Moreover, future research endeavors may delve into the exploration of non-linear controllers, such as sliding mode or model predictive controllers, to tackle the inherent non-linearities within the system. This avenue of research holds the promise of deepening our understanding and uncovering the most efficient controller strategies tailored for half-bridge DC-DC buck converters.

CHAPTER 4
DESIGIN AND MODELLING OF NOVEL SIDO BOOST/BUCK DC-DC CONVERTER

4.1 INTRODUCTION

POWER CONVERTER Single-input–multiple-output (SIMO) dc–dc converter stages have been utilized in variety of applications, architectures having multiple dc ports.[14] Typical examples include electric vehicles Charger. And auxiliary supplies like LED drivers, MOSFET Gate driver, controlling IC driver as well as stand-by power supplies To ensure the effective functioning of systems employing multiple outputs, it is imperative to establish seamless coordination of control among each converter, facilitating optimal power flow management The approach of employing N distinct single-input-single-output (SISO) DC-DC converters to generate N outputs results in enlarged dimensions, increased volume, and elevated expenses. Hence, in pursuit of cost reduction, size minimization, and the attainment of high-power density, the proposition of single-input multiple-output DC-DC converters (SIMO) has emerged [13]-[18]. These converters aim to reduce costs, decrease size, and achieve high power density This study introduces a non-isolated Single-Input-Dual-Output (SIDO) DC-DC converter capable of delivering both step-up and multiple step-down outputs from a singular DC input. The design achieves this by substituting the control switch of a boost converter topology with series-connected switches, leveraging the resultant switch nodes to optimize supplementary outputs through low-pass filter networks The step-up and step-down gains obtained are equivalent to those of individual boost and buck converters, respectively. However, in contrast to separate converters, the proposed configuration employs a smaller number of switching elements [19]-[24]. Additionally, the converter maintains continuous currents at both the input and the step-down output. Consequently, the demand for input filtering is reduced compared to a conventional buck or buck-boost converter. Moreover, the complementary switching operation does not necessitate dead-time protection, thanks to the built-in safeguarding provided by the circuit topology. A further point to consider is that the control system of the SIDO converter is comparable to that of

traditional buck and boost converters. In light of the fact that these two items are equivalent, it is not difficult to expand control procedures in order to accomplish accurate regulation of each output. When it comes to applications like as solar-battery chargers, DC nano grids, and bias supplies, where several outputs at different voltage levels are needed, this versatility is crucial. A small signal analysis is conducted for the single-input, dual-output (SIDO) step-up and step-down converter, taking into account variations in both the input voltage and the load.

In order to function properly, modern electronic systems require the supply of multiple direct current (dc) outputs that are different in voltage. Additionally, additional circuits, which are referred to as auxiliary circuits, are typically located next to the primary power stage. The operation of these circuits is dependent on low voltages, as is the case in fuel cell systems. It is possible for the converter that has been suggested to deliver a greater output voltage, which functions as the major power stage, in addition to a secondary output that has a lower voltage. Numerous applications, including solar-battery chargers, DC nano grids, bias supplies, and others, could potentially benefit from the converter [25]-[28].

4.2 MODELLING OF SIDO CONVERTER

A sixth-order non-isolated SIDO converter is composed of two switches, Sw_1 and Sw_2. The schematic diagram of the SIDO, having dual dc outputs as shown in Fig.1., focuses on continuous conduction mode (CCM) of operation, all the subsequent analysis in this work would consider this assumption. The SIDO converter is implemented with two bidirectional switches, Sw_1 and Sw_2. These switches create four operating modes, with three being distinct, thus results in three different switching mode of the converter. These modes are discussed in the following sections:

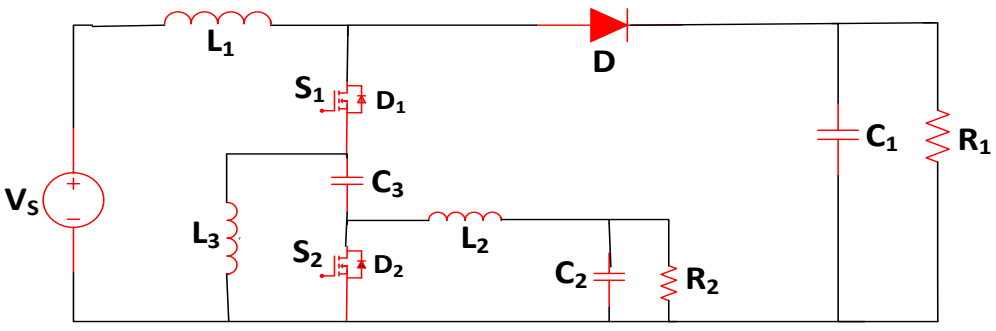

Fig 4.1 SIDO Converter Circuit Diagram

4.2.1 MODE 1 OF OPERATION

When Both Sw_1 and Sw_2 are on as shown in Fig.4.2 this interval. The inductor L_1 charged up, while the inductor L_2 discharge through switch Sw_2 and inductor L_3 discharge through source. the waveforms of the inductor current with respect to switching intervals D_2.

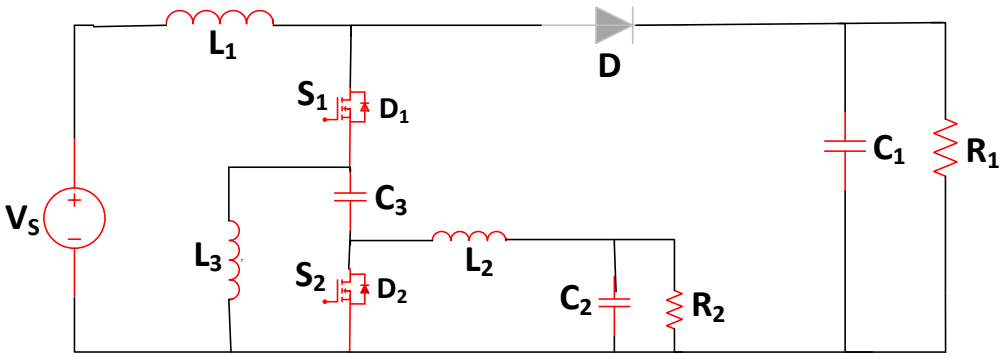

Fig 4.2: Mode 1 Circuit Diagram of SIDO Converter

Considering the DC loads R_1 and R_2 at the step-up and step-down terminals, respectively, the differential equation for the different inductor currents and the capacitor voltages are:

$$\frac{di_{L_1}}{dt} = \frac{V_s}{L_1} + \frac{V_{C_3}}{L_1} \quad (4.1)$$

$$\frac{di_{L_2}}{dt} = -\frac{V_{C_2}}{L_2} \quad (4.2)$$

$$\frac{di_{L_3}}{dt} = -\frac{V_{C_3}}{L_3} \quad (4.3)$$

$$\frac{dV_{C_1}}{dt} = \frac{V_{C_1}}{C_1 R_1} \quad (4.4)$$

$$\frac{dV_{C_2}}{dt} = \frac{i_{L_2}}{C_2} - \frac{V_{C_2}}{C_2 R_2} \quad (4.5)$$

$$\frac{dV_{C_3}}{dt} = \frac{i_{L_3}}{C_3} - \frac{i_{L_1}}{C_3} \quad (4.6)$$

4.2.2 MODE 2 OF OPERATION:

During this mode the inductor L_1 charge is distributed in components: one is flowing through diode D, and another one is through the buck inductor L_2.

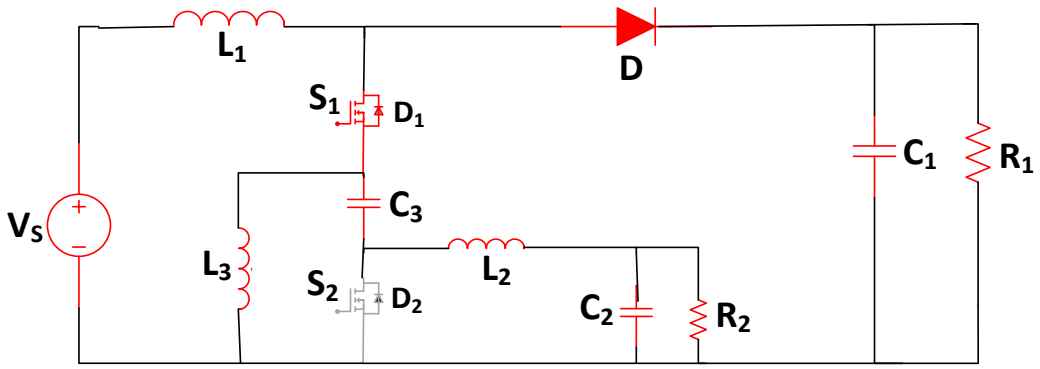

Fig 4.3 Mode 2 Circuit Diagram of SIDO Converter

The step-up and step-down converter draws energy from the source during this mode. the differential equation for the different inductor currents and the capacitor voltages are:

$$\frac{di_{L_1}}{dt} = \frac{V_s}{L_1} - \frac{V_{C_1}}{L_1} \tag{4.7}$$

$$\frac{di_{L_2}}{dt} = \frac{V_{C_1}}{L_2} - \frac{V_{C_2}}{L_2} + \frac{V_{C_3}}{L_2} \tag{4.8}$$

$$\frac{di_{L_3}}{dt} = \frac{V_{C_1}}{L_3} \tag{4.9}$$

$$\frac{dV_{C_1}}{dt} = \frac{i_{L_1}}{C_1} - \frac{i_{L_2}}{C_1} - \frac{i_{L_3}}{C_1} - \frac{V_{C_1}}{R_1} \tag{4.10}$$

$$\frac{dV_{C_2}}{dt} = \frac{i_{L_2}}{C_2} - \frac{V_{C_2}}{C_2 R_2} \tag{4.11}$$

$$\frac{dV_{C_3}}{dt} = -\frac{i_{L_2}}{C_3} \tag{4.12}$$

4.2.3 MODE 3 OF OPERATION:

In this mode, the inductor L_2 discharge through antiparallel diode D_2 of switch S_2. the waveforms of the inductor current with respect to switching intervals($1-D_1$) shown in Fig.4.4.

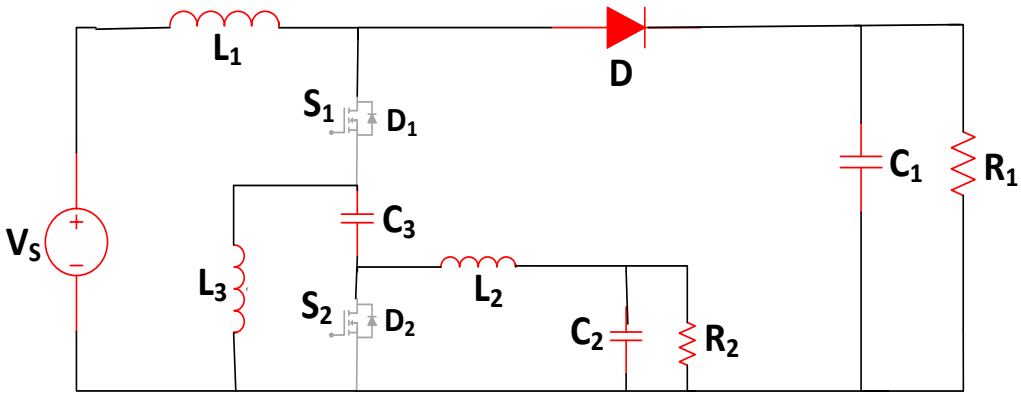

Fig 4.4 Mode 3 Circuit Diagram of SIDO Converter

The differential equation for the different inductor currents and the capacitor voltages are:

$$\frac{di_{L_1}}{dt} = \frac{V_s}{L_1} - \frac{V_{C_1}}{L_1} \tag{4.13}$$

$$\frac{di_{L_2}}{dt} = -\frac{V_{C_2}}{L_2} \tag{4.14}$$

$$\frac{di_{L_3}}{dt} = -\frac{V_{C_3}}{L_3} \tag{4.15}$$

$$\frac{dV_{C_1}}{dt} = \frac{i_{L_1}}{C_1} - \frac{V_{C_1}}{C_1 R_1} \tag{4.16}$$

$$\frac{dV_{C_2}}{dt} = \frac{i_{L_2}}{C_2} - \frac{V_{C_2}}{C_2 R_2} \tag{4.17}$$

$$\frac{dV_{C_3}}{dt} = \frac{i_{L_3}}{C_3} \tag{4.18}$$

The analysis of the switching waveform of the Single-Inductor Dual-Output (SIDO) Boost converter elucidates three distinct operational modes, each delineating specific configurations and behaviors of the converter's key components. Mode 1, characterized by the concurrent activation of both switches, initiates a charging phase where the inductor begins accumulating energy, while inductors L2 and L3 discharge energy to their respective output loads. Notably, during this mode, the diode remains inactive, ensuring controlled energy flow dynamics. Transitioning to Mode 2, which

occurs when switch 1 is activated while switch 2 is deactivated, all three inductors undergo a charging cycle simultaneously, with the diode assuming a conductive state, facilitating directed current flow. Finally, Mode 3, marked by the deactivation of both switches, signifies a phase where all three inductors discharge stored energy, while the diode maintains a conductive state, ensuring continuous current flow. This detailed analysis provides valuable insights into the operational modes of the SIDO Boost converter, essential for understanding its energy conversion mechanisms and optimizing performance across varying load conditions. The switching waveform of the SIDO Boost converter can be seen in Fig.3:

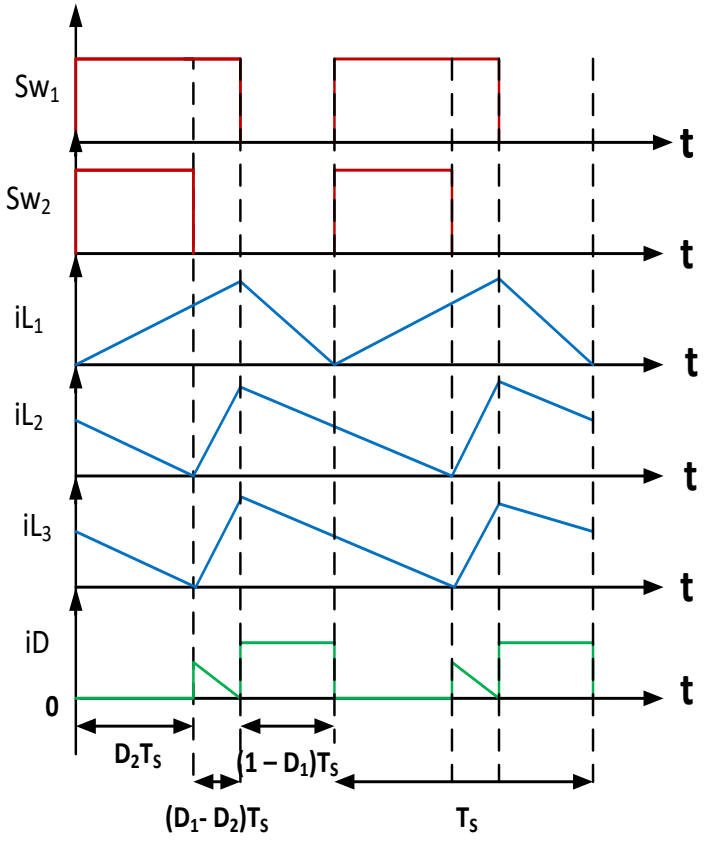

Fig.4.5 Switching Waveform with respect to mode of operations.

4.3 SMALL SIGNAL MODELING

Small signal modelling of SIDO converter is carried out using the state space averaging technique. The converter modelling is analyzed with the following presumptions. Both output voltage and current are constant in a steady state condition. Switch parasitic capacitance C_o can be ignored. The components inductor and

capacitor does not have any series resistance. An analysis of circuit dynamics is conducted by deriving a small-signal model from the circuit equation. All the inductor current and all capacitor voltage are state variables. Input voltage, output voltage are controlled input variable and output variable respectively of the SIDO converter as shown in Eq. (19).

$$x = \left[i_{L_1}\, i_{L_2}\, i_{L_3}\, V_{C_1}\ V_{C_2}\, V_{C_3}\right], \quad u = [V_s], \quad y = [V_o] \tag{4.19}$$

The subsequent equation presents the state space representation of a converter system:

$$\begin{aligned} \dot{x} &= Ax + Bu \\ y &= Cx + Du \end{aligned} \tag{4.20}$$

where A is the state transition matrix, B is the input matrix, C is the output matrix and D is the direct transmission matrix.

One method to reduce the effect of the switching ripple on the circuit equations is to average across one switching interval. The averaged switching model is obtained by calculating the average of the aforementioned equations over a single switching period according to Eq. (4.19) – Eq. (4.20)

$$A = A_1 d_2 + A_2(d_1 - d_2) + A_3(1 - d_1) \tag{4.21}$$

$$B = B_1 d_2 + B_2(d_1 - d_2) + B_3(1 - d_1) \tag{4.22}$$

$$C = C_1 d_2 + C_2(d_1 - d_2) + C_3(1 - d_1) \tag{4.23}$$

$$D = D_1 d_2 + D_2(d_1 - d_2) + D_3(1 - d_1) \tag{4.24}$$

$$d = D + \hat{d}\ \ x = X + \hat{x}\, u = U + \hat{u}\, y = Y + \hat{y} \tag{4.25}$$

Small signal model is linearized by introducing the perturbed variables into the averaged state-space model Eq. (4.21) – Eq. (4.25) while disregarding the higher order terms.

$$\hat{x}(s) = A\hat{x}(s) + B\hat{u}(s) + \Big(\big(A_1\hat{d}_2 - A_2(\hat{d}_1 - \hat{d}_2\big) - A_3\hat{d}_1)\, X(s) + \big(B_1\hat{d}_2 - B_2(\hat{d}_1 - \hat{d}_2\big) - A_3\hat{d}_1)\, U(s)\Big) \tag{4.26}$$

The control to output transfer function can be derived using Eq. (4.26) as shown below:

$$\frac{\widehat{V_1}(s)}{\widehat{d_1}(s)}, \frac{\widehat{V_2}(s)}{\widehat{d_1}(s)} \quad when \;\; \hat{d}_2 = 0, \hat{u} = 0 \tag{4.27}$$

$$\frac{\hat{X}(s)}{\hat{d}(s)} = (sI - A)^{-1}\left((A_2 - A_3)\, X(s) + (B_2 - B_3)\, U(s)\right) \tag{4.28}$$

$$\frac{\hat{V}_1}{\widehat{d_1}} = \frac{\alpha_{15}s^5 - \alpha_{14}s^4 - \alpha_{13}s^3 - \alpha_{12}s^2 - \alpha_{21}s + \alpha_{20}}{\beta_6 s^6 + \beta_5 s^5 + \beta_4 s^4 + \beta_3 s^3 + \beta_2 s^2 + \beta_1 s + \beta_0} \tag{4.29}$$

The constant values are provided as follows:

$\alpha_{15} = 3.957 \times 10^4$ $\quad \alpha_{14} = 3.62 \times 10^8$ $\quad \alpha_{13} = 1.925 \times 10^{12}$
$\alpha_{12} = 2.686 \times 10^{15}$ $\quad \alpha_{11} = 1.562 \times 10^{19}$ $\quad \alpha_{10} = 9.271 \times 10^{22}$
$\beta_5 = 1108$ $\quad \beta_4 = 4.161 \times 10^7$ $\quad \beta_3 = 2.884 \times 10^{10}$
$\beta_2 = 4.87 \times 10^{14}$ $\quad \beta_1 = 1.317 \times 10^{17}$ $\quad \beta_0 = 1.129 \times 10^{21}$

Similarly,

$\frac{\widehat{V_1}(s)}{\widehat{d_2}(s)}$ can be calculated when $\hat{d}_1 = 0 \; and \; \hat{u} = 0$
$\frac{\widehat{V_2}(s)}{\widehat{d_2}(s)}$ can be calculated when $\hat{d}_1 = 0 \; and \; \hat{u} = 0$ (4.30)

$$\frac{\hat{X}(s)}{\hat{d}(s)} = (sI - A)^{-1}\left((A_1 - A_2)\, X(s) + (B_1 - B_2)\, U(s)\right) \tag{4.31}$$

$$\frac{\hat{V}_2}{\widehat{d_2}} = \frac{\alpha_{24}s^4 - \alpha_{23}s^3 - \alpha_{22}s^2 - \alpha_{21}s - \alpha_{20}}{\beta_6 s^6 + \beta_5 s^5 + \beta_4 s^4 + \beta_3 s^3 + \beta_2 s^2 + \beta_1 s + \beta_0} \tag{4.32}$$

The constant values are specified as follows:

$\alpha_{24} = 1.489 \times 10^9$ $\quad \alpha_{23} = 3.708 \times 10^{11}$ $\quad \alpha_{22} = 3.655 \times 10^{16}$
$\alpha_{21} = 7.34 \times 10^{18}$ $\quad \alpha_{20} = 9.481 \times 10^{22}$ $\quad \beta_6 = 1$
$\beta_5 = 1108$ $\quad \beta_4 = 4.161 \times 10^7$ $\quad \beta_3 = 2.884 \times 10^{10}$
$\beta_2 = 4.87 \times 10^{14}$ $\quad \beta_1 = 1.317 \times 10^{17}$ $\quad \beta_0 = 1.129 \times 10^{21}$

In the analysis of a single-inductor dual-output (SIDO) boost converter, the transfer functions show notable characteristics. The self-regulation metrics (V1/D1) reveal

gain margin of 32.04 dB with a phase margin of -120degrees, while V2/D2 boasts an infinite gain margin and a30-degree phase margin, indicating robust stability. Cross-regulation effects, quantified by off-diagonal components, exhibit a gain margin of 26.02 dB and -20 degrees phase for V1/D2, and 27.95 dB with -140 degrees phase for the counterpart, highlighting the intricate balance of performance across outputs as shown in Fig.4.6 and Fig.4.7

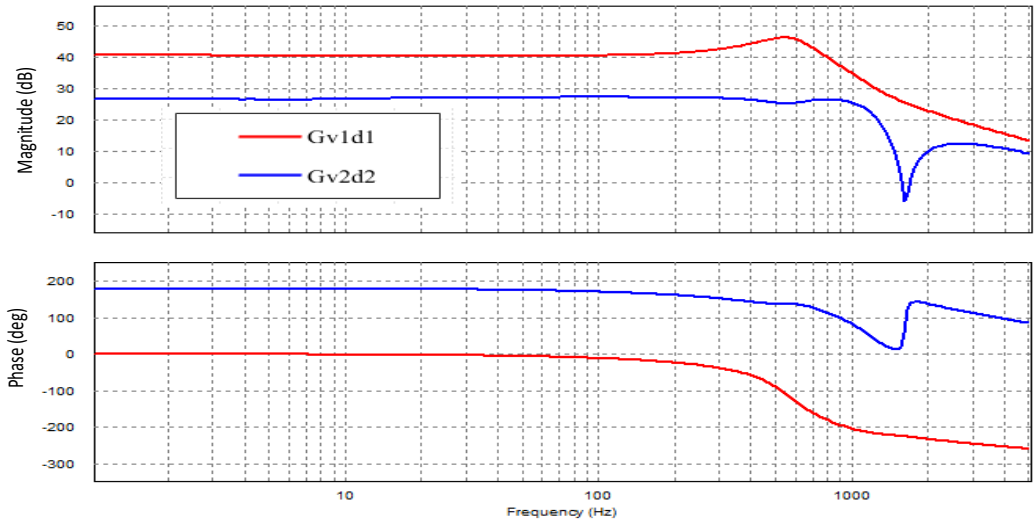

Fig 4.6. Open loop frequency response of the system diagonal elements.

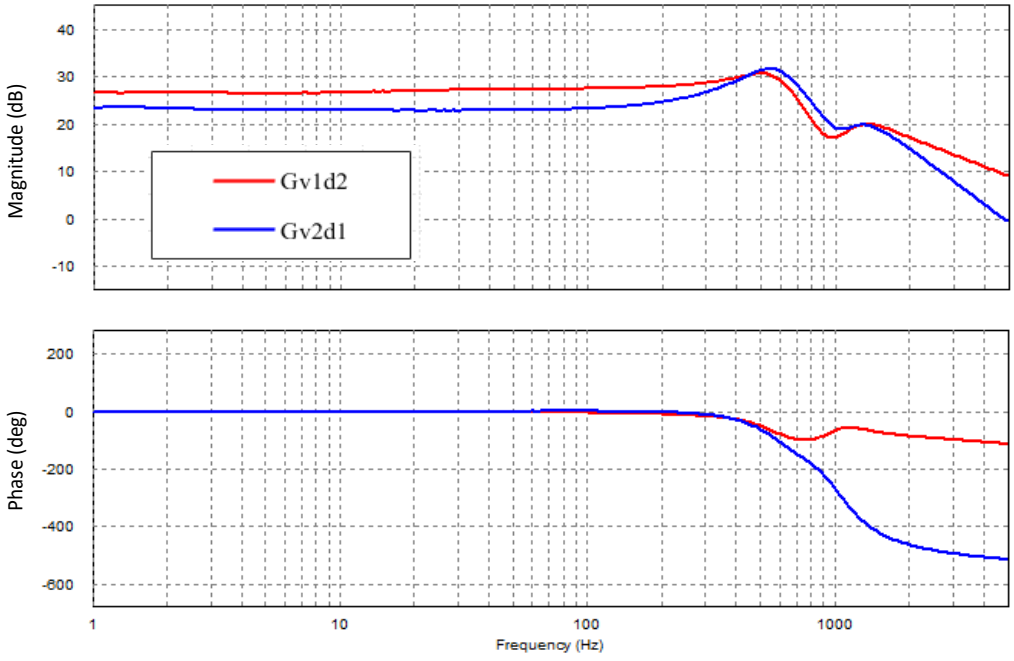

Fig 4.7 Open loop frequency response of the system off diagonal elements.

Table I Design parameter of SIDO converter

Parameters	Symbols	Values
Input Voltage	V_s	48 V
Output Voltage	V_1	96 V
Output Voltage	V_2	12V
Switching Frequency	f_{sw}	20 kHz
Inductors	L_1, L_2, L_3	1.2µH
Capacitors	C_1, C_2, C_3	47µF
Load Resistance	R_1	96Ω
Load Resistance	R_2	12Ω

CHAPTER 5
CONTROL METHODOLOGY IN SIDO CONVERTER

5.1 INTRODUCTION

For the SIDO converter to achieve the desired voltage regulation, improve dynamic response, voltage gain and increase system stability, closed-loop control must be used. The study employed a proportional integral (PI) controller in closed-loop SIDO converters with voltage mode control is thoroughly studied, and its effects on the converter's overall performance are evaluated

5.2 CLOSED LOOP CONTROL

Closed-loop control is essential for maintaining stable and accurate voltage outputs in a Single Input Double Output (SIDO) boost converter. This is critical for the efficient operation of voltage-sensitive electronic equipment.

Any electrical system, especially those involving power conversion like a SIDO boost converter, fluctuations in input voltage or changes in load demand can cause unwelcome changes in output voltage. Such variations may compromise the operation of converter-powered devices or potentially destroy delicate components. By always tracking the output voltage and matching it with a target setpoint voltage, closed-loop control systems help to solve this problem. Should a disagreement be found, the system automatically modulates its operation to offset the variation, therefore guaranteeing the stability and within range of output voltage. Maintaining constant performance under changing running conditions depends critically on this dynamic, real-time adjusting capability.

Using a Proportional-Integral (PI) controller inside a closed-loop control system provides a sophisticated method for SIDO boost converter output voltage management. Reacting to the instantaneous difference (error) between the actual output voltage and the desired setpoint, the proportional section of the PI controller It guarantees fast response to any changes by matching the operation of the converter to this error. But the proportional control by itself may produce a residual steady-state error, in which case the integral component becomes rather important. Consistent long-

term accuracy depends on the integral portion accumulating the error over time applying a correction to eliminate the steady-state error. For voltage control in boost converters, this dual-action approach results in quite effective PI controller.

5.3 VOLTAGE MODE CONTROL OF SIDO BOOST CONVERTER

Specifically, voltage mode control is the technique whereby the control system employs the output voltage as the main feedback to control the running of the converter. Since the control loop of this straightforward and effective approach concentrates only on reducing the voltage error, it guarantees the intended voltage output. Voltage mode control guarantees that each output of a SIDO boost converter under the control of a PI controller maintains its set voltage level independent of input fluctuations or load changes. It is especially helpful since it can be immediately applied with a PI controller to give fast and accurate voltage change and simplifies the control approach.

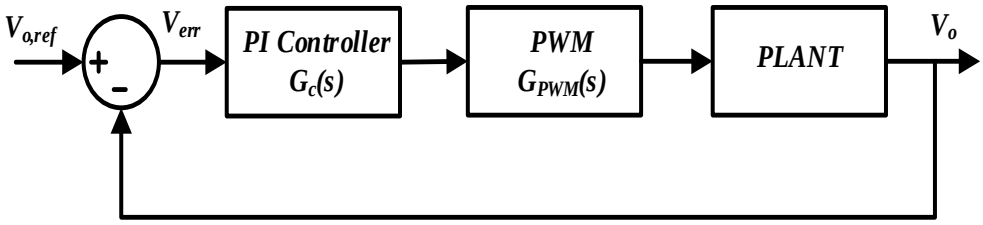

Fig. 5.1Closed loop voltage mode control of SIDO converter

The transfer function of the PI controller is given by:

$$G_1(s) = K_{prop} + \frac{K_{int}}{s} \tag{5.1}$$

$$G_1(s) = 0.0015 + \frac{1.2224}{s} \tag{5.2}$$

$$G_2(s) = K_{prop} + \frac{K_{int}}{s} \tag{5.3}$$

$$G_2(s) = 0.0017 + \frac{1.9406}{s} \tag{5.4}$$

Where,

$G_1(s)$ = PI Transfer function for controlling the boost output voltage

$G_2(s)$ = PI Transfer function for controlling the buck output voltage

5.4 SIMULATION RESULTS

The SIDO converter was analyzed using MATLAB/Simulink modelling and simulation techniques as shown in the fig. Different inputs and load conditions were applied to examine the behaviors of these systems in both open and closed loop configurations.

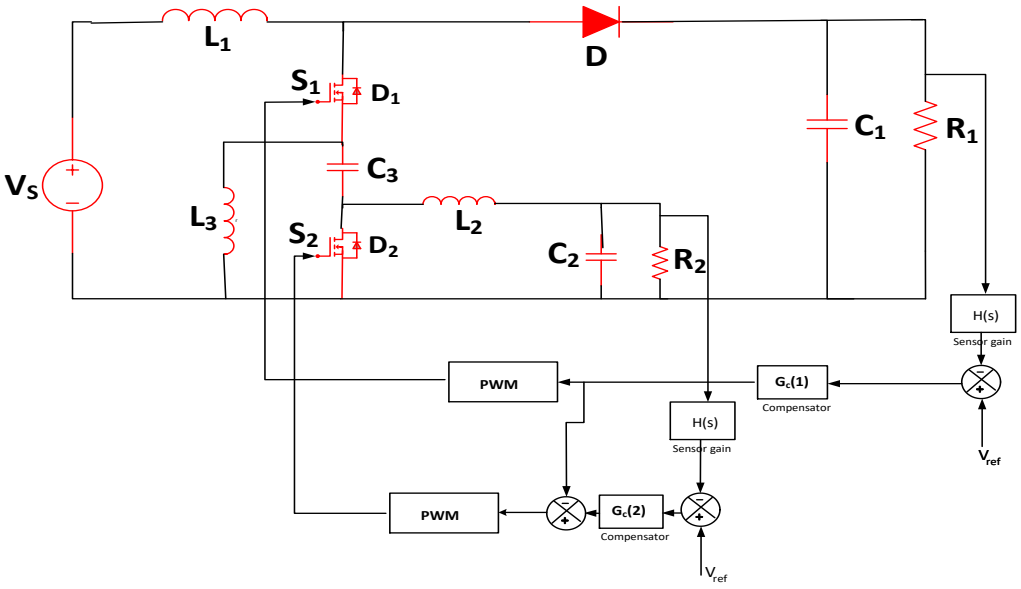

Fig 5.2 Block diagram for closed loop of SIDO converter

1.1.1

Table II Performance parameters for SIDO Converter

DUTY	AVERAGE VOLTAGE		PEAK OVERSHOOT		SETTLING TIME	
	V_1	V_2	V_1	V_2	V_1	V_2
$D_1 = 0.6$ $D_2 = 0.4$	105.0V	13.42V	60.1%	162%	13 ms	13.3 ms
$D_1 = 0.5$ $D_2 = 0.4$	85.4V	9.40V	65.9%	190%	12.5 ms	9.28ms
$D_1 = 0.6$ $D_2 = 0.3$	105.9V	14.22V	50.8%	142%	13.08 ms	13.1 ms
$D_1 = 0.5$ $D_2 = 0.3$	83.7V	10.95V	61.9%	145%	12.2 ms	13.2 ms

5.4.1 OPEN LOOP OUTPUT VOLTAGE RESPONSE:

Optimizing the performance of a Single Input Double Output (SIDO) boost converter depends critically on an awareness of the output voltage response with respect to changes in the duty cycle. The output voltage and efficiency of converters depend much on the duty cycle—that is, the percentage of one period in which a signal or system is active.

In the experiment described, the SIDO boost/buck converter was tested with various duty cycles to analyze the resulting output voltages. Applying different duty cycles to Switch 1 and Switch 2 in an open-loop system resulted in noticeable differences in both the transient and steady-state responses. More precisely, the converter's boost section exhibited a transient response with a peak overshoot of 168 V when subjected to a duty cycle of 0.6. Eventually, it settled at a steady-state output voltage of 107 V. On the other hand, the buck section, with a duty cycle of 0.4, had a relatively smaller peak overshoot of 35 V and eventually stabilized at a steady-state value of 13.5 V.

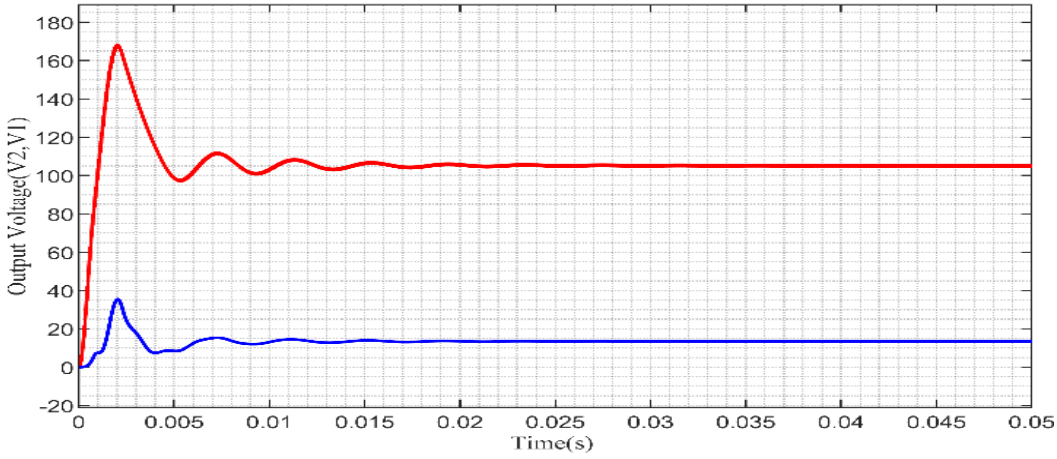

Fig. 5.3 Open loop output voltage at $d_1 = 0.6$ & $d_2 = 0.4$

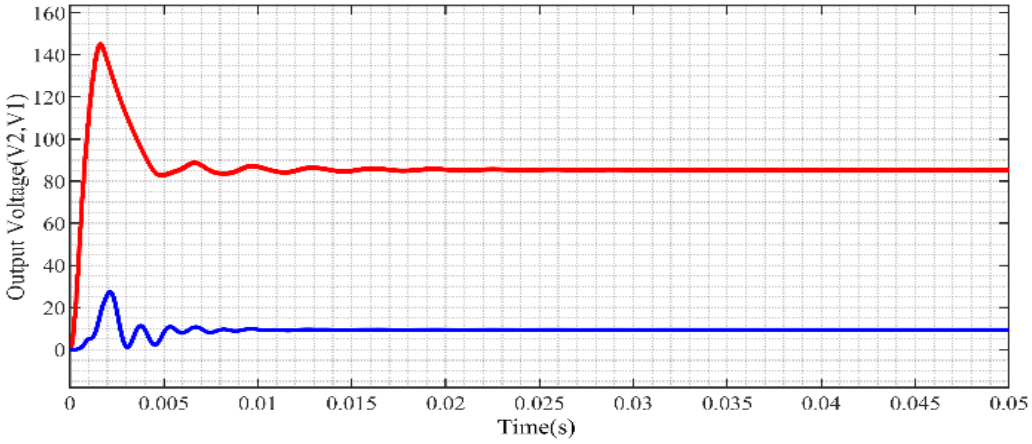

Fig. 5.4 Open loop output voltage at $d_1 = 0.5$ & $d_2 = 0.4$

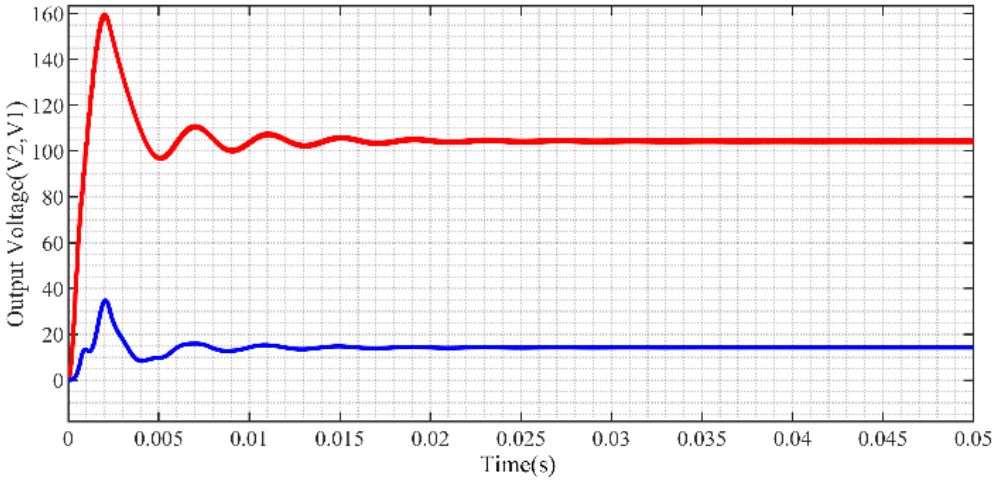

Fig. 5.5 Open loop output voltage at $d_1 = 0.6$ & $d_2 = 0.3$

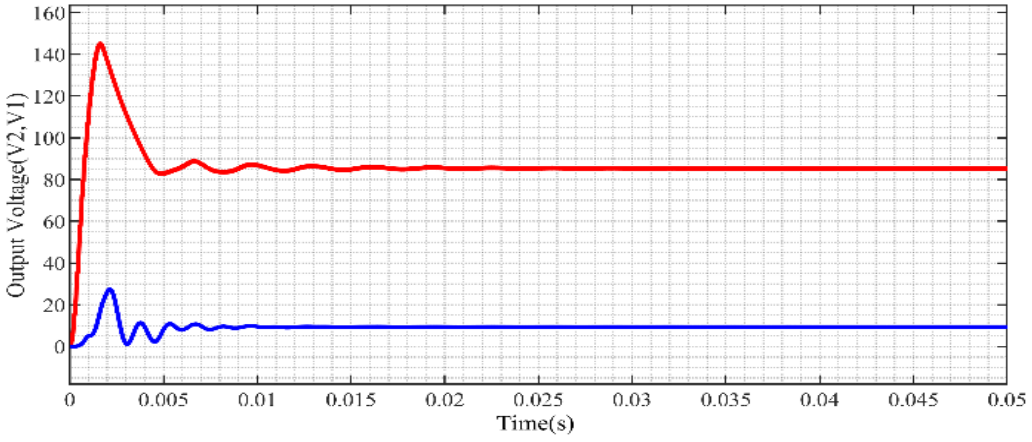

Fig 5.6 Open loop output voltage at $d_1 = 0.5$ & $d_2 = 0.3$

These observations highlight the importance of carefully adjusting the duty cycle settings of the SIDO boost converter. It is evident that even slight changes in the duty cycle can significantly impact the converter's voltage and current dynamics. The peak overshoot during the transient phase highlights the importance of meticulous duty cycle selection to avoid possible overvoltage stress on connected devices and to guarantee the converter's efficiency and longevity

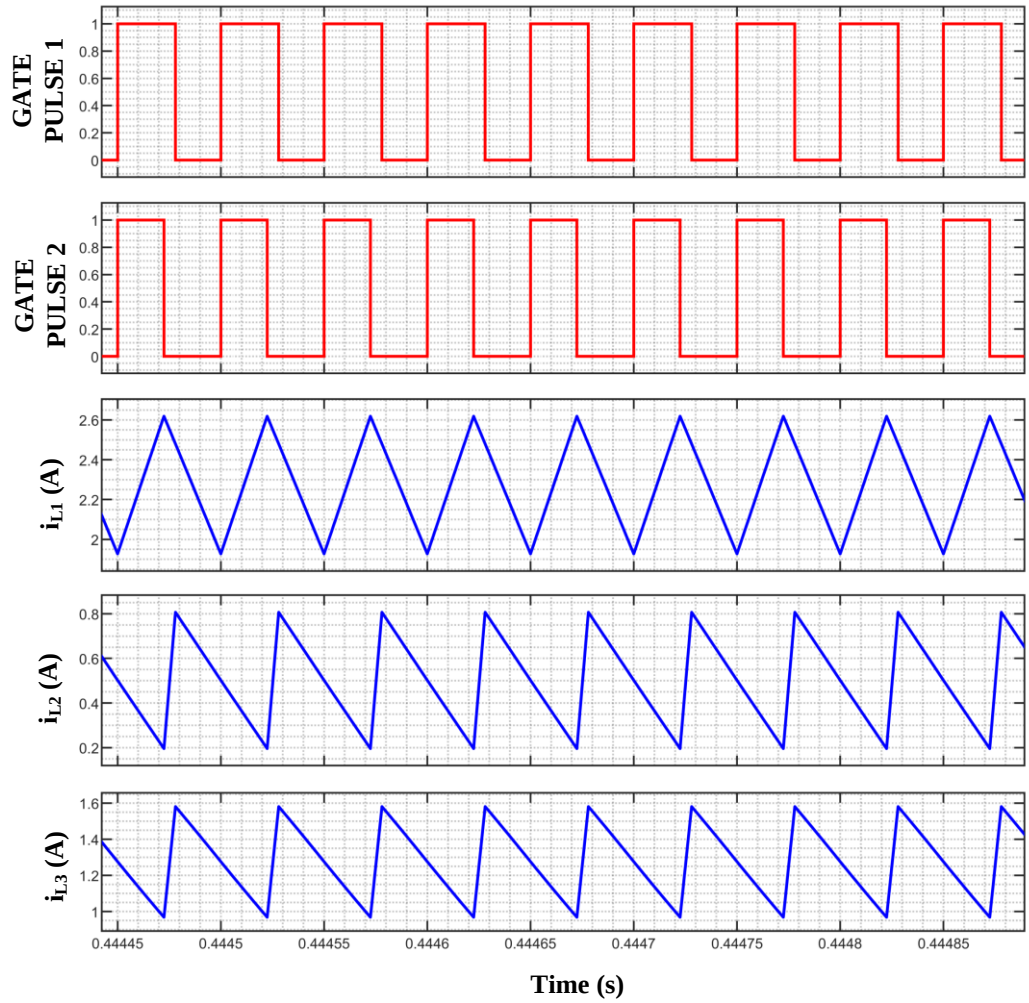

Fig. 5.7 Inductor current waveform with respect to gate pulse

Moreover, when assessing the performance of each inductor current and capacitor voltage, unique profiles become apparent. Every component in the converter responds uniquely to changes in duty cycle, which reflects their function in stabilizing voltage and current fluctuations. Inductors and capacitors play a crucial role in stabilizing the output after the initial transient overshoot. Inductors resist changes in current, while capacitors store and release charge, collectively contributing to the stabilization

process. More precisely, the current profile of the inductor shows a clear connection to variations in duty cycle. When the duty cycle is increased, it usually leads to a higher current in the inductor, which in turn contributes to the observed peak overshoot in output voltage. Meanwhile, the voltage profile of the capacitor has a direct impact on the phase of smoothing out, which helps the system reach a steady state.

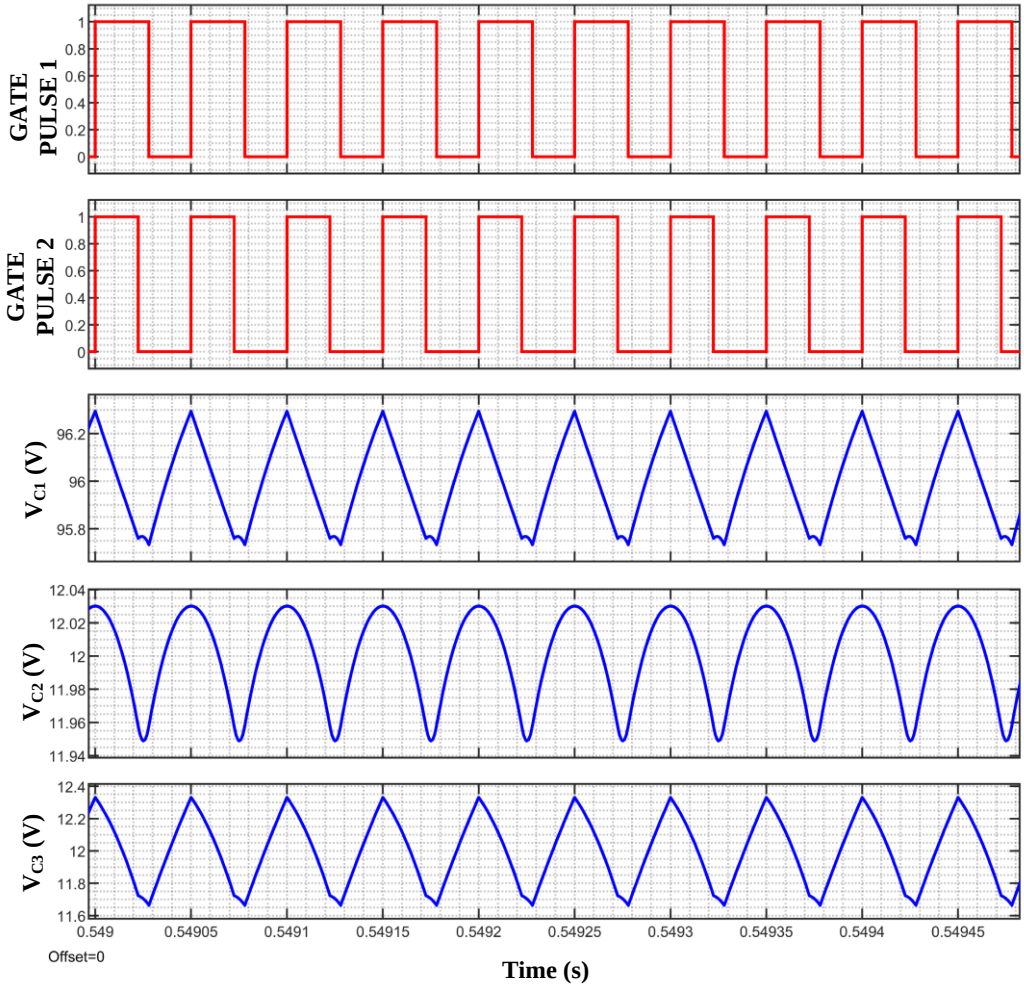

Fig. 5.8 Capacitor voltage waveform with respect to gate pulse

5.4.2 SELF AND CROSS-REGULATION:

In DC-DC converters, regulation refers to the ability to maintain a constant output voltage despite variations in input voltage or load conditions. This regulation can be classified into self-regulation and cross-regulation:

1. **Self-Regulation**: This pertains to the converter's capacity to stabilize its own output voltage in response to changes in its input voltage or load. In a well-designed

DC-DC converter, feedback control mechanisms are employed to adjust the duty cycle of the switching elements, thereby ensuring that the output voltage remains within specified limits. The feedback loop continuously monitors the output and makes real-time adjustments to counteract any deviations caused by fluctuations in the input supply or changes in the load demand.

2. **Cross-Regulation**: This occurs in multi-output DC-DC converters and refers to the impact that changes in one output have on the other outputs. Ideally, each output should remain stable regardless of variations in the other outputs; however, due to interactions within the shared components of the converter, such as the transformer or the control circuitry, changes in one output can influence the stability and regulation of the other outputs. Effective cross-regulation minimizes this interaction, ensuring that each output maintains its intended voltage independently of the conditions affecting the other outputs. This is typically achieved through careful design and placement of feedback loops for each output, as well as through the use of isolated regulation techniques and improved circuit topologies.

The impact of self- and cross-regulation on the SIDO converter is seen in Fig 5.8. At 0.25 seconds, a sudden change in R_1 results in a self-regulation of 1.2 V in the boost output voltage V_1. The cross-regulation of the buck output voltage is measured to be 500 mV.

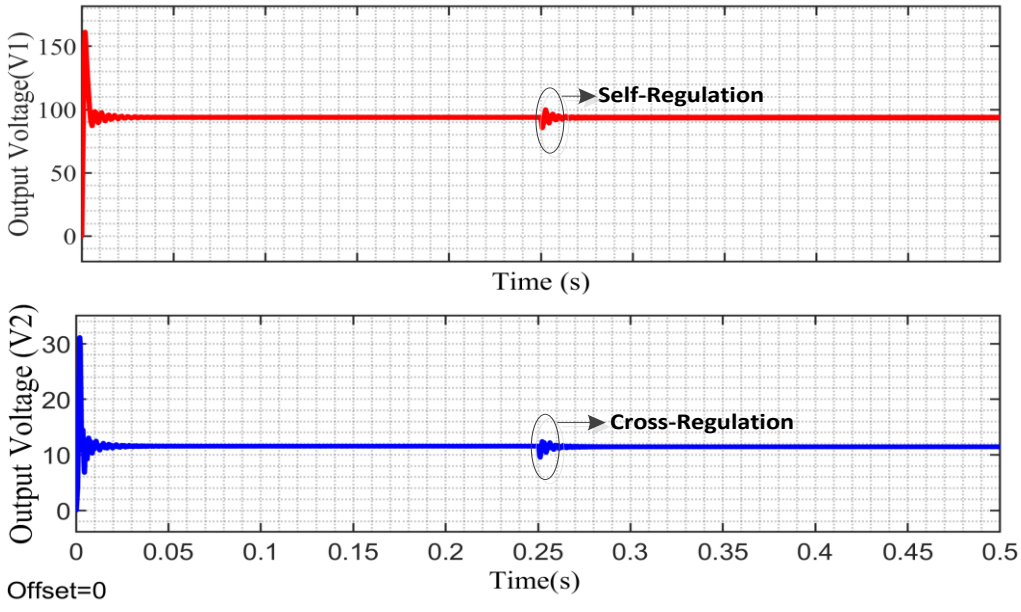

Fig 5.9. Regulation effect on the open loop output voltage

The effect on the SIDO converter of self- and cross-regulation is seen in Fig. 5.9. At 0.25 seconds, a significant shift in R_2 results in a self-regulation of 600 mV in the buck output voltage V_2 and a cross-regulation of 400mV in the boost output voltage.

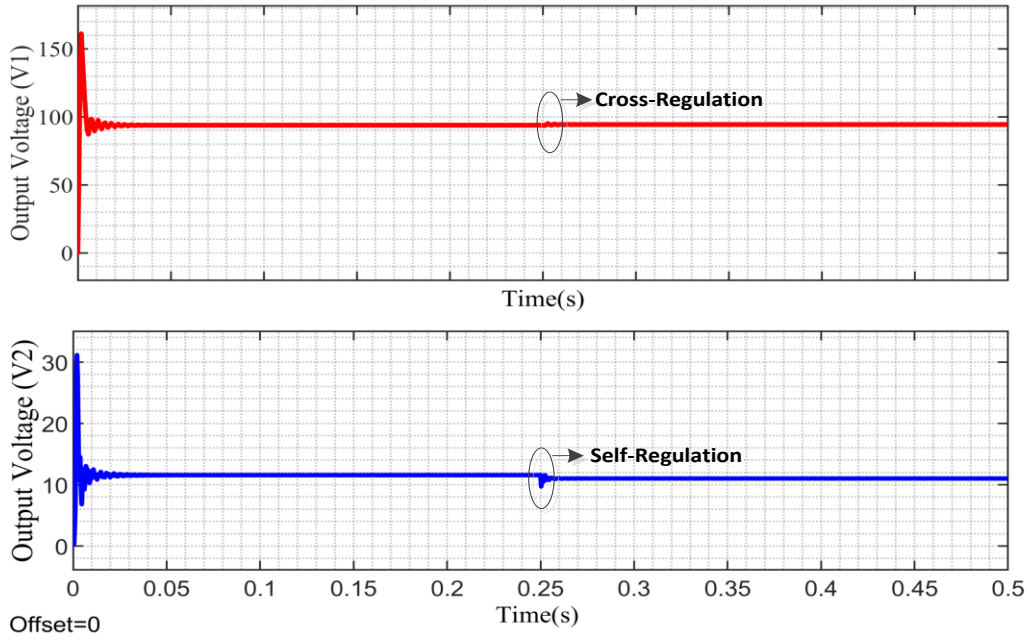

Fig 5.10 Regulation effect on the open loop output voltage

This shows that in SIDO converter with a change in load R_1 and R_2 there is effect on both transient and steady state.

5.4.3 OUTPUT VOLTAGE PERFORMANCE UNDER CLOSED LOOP.

After implementing closed-loop control in the converter, the output voltages become stable, with the boost voltage maintaining a steady 96 V and the buck voltage stabilizing at 12 V. The peak overshoot observed in the output voltages is significantly reduced compared to the open-loop mode, as illustrated in Figure 5.11. This improvement demonstrates the effectiveness of the closed-loop control in enhancing the system's transient response and stability seen in Fig 5.11

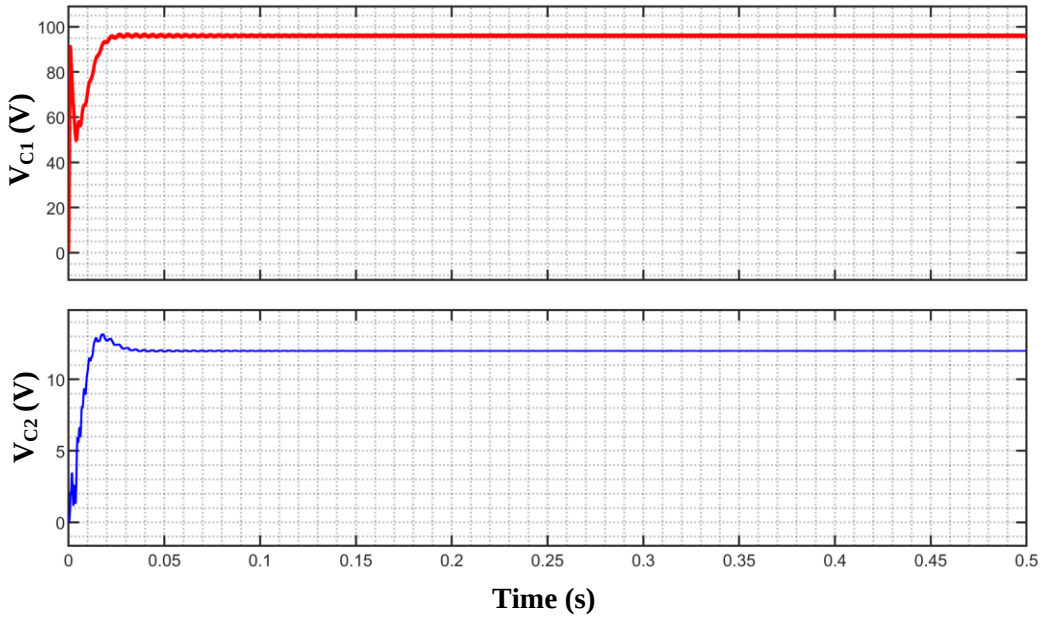

Fig.5.11 Closed Loop Output Voltage

5.4.4 LOAD REGULATION:

Load regulation in a DC-DC converter refers to the ability of the converter to maintain a stable output voltage as the load varies. It is a measure of the converter's performance in providing a constant voltage to the load despite changes in the current drawn by the load. Mathematically, load regulation is often expressed as a percentage and is defined as the difference in output voltage from no load to full load, relative to the nominal output voltage In practical terms, good load regulation means that the output voltage varies minimally as the load current changes from its minimum to maximum value. This is achieved through the use of feedback control mechanisms within the DC-DC converter. The feedback system continuously monitors the output voltage and adjusts the converter's operation, such as the duty cycle of the switching elements, to correct any deviations from the desired output voltage. Effective load regulation is crucial for applications where a stable voltage is required despite varying power demands, such as in sensitive electronic devices, communication systems, and precision instrumentation. It ensures the reliable operation of the load and protects it from voltage fluctuations that could cause malfunction or damage.

In a Single Input Double Output (SIDO) boost converter experiment focusing on load regulation, a notable observation was made when the boost resistance was adjusted from 96 ohms to 72 ohms at (t = 0.5) seconds. Following this adjustment, the output voltage swiftly stabilized with minimal oscillations, settling within a mere 13 ms. Remarkably, the overshoot was limited to just 3%, underscoring the system's robust response to changes in load. Conversely, under the same load variation, the buck output demonstrated a slightly longer settling time of 19 ms, accompanied by a higher overshoot of 10%. This disparity highlights the differing dynamic responses of the boost and buck outputs to load variations within the converter, reflecting the intricacies of managing multiple outputs in a SIDO configuration.

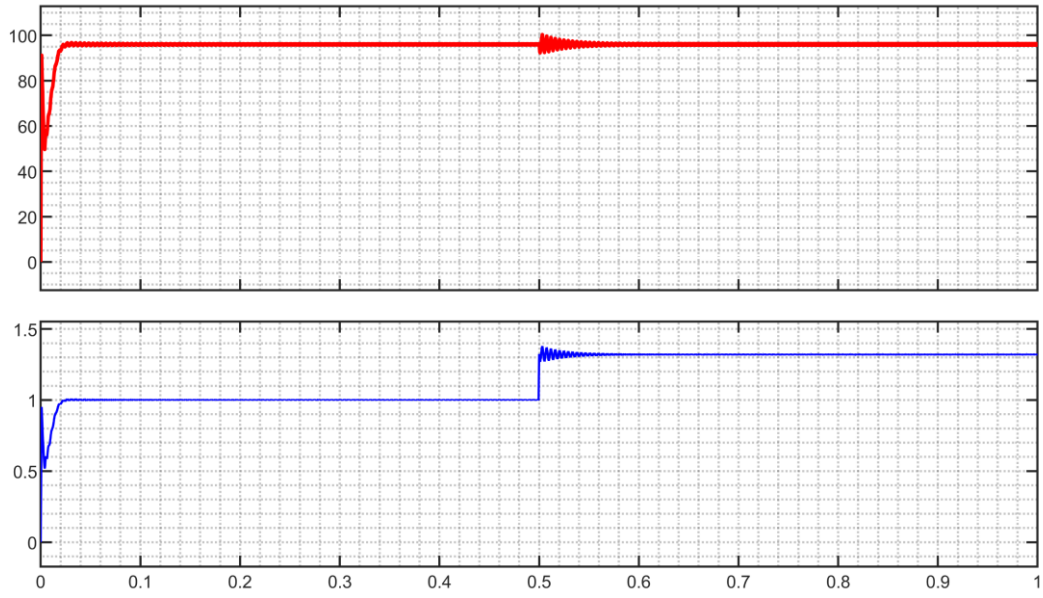

(a)

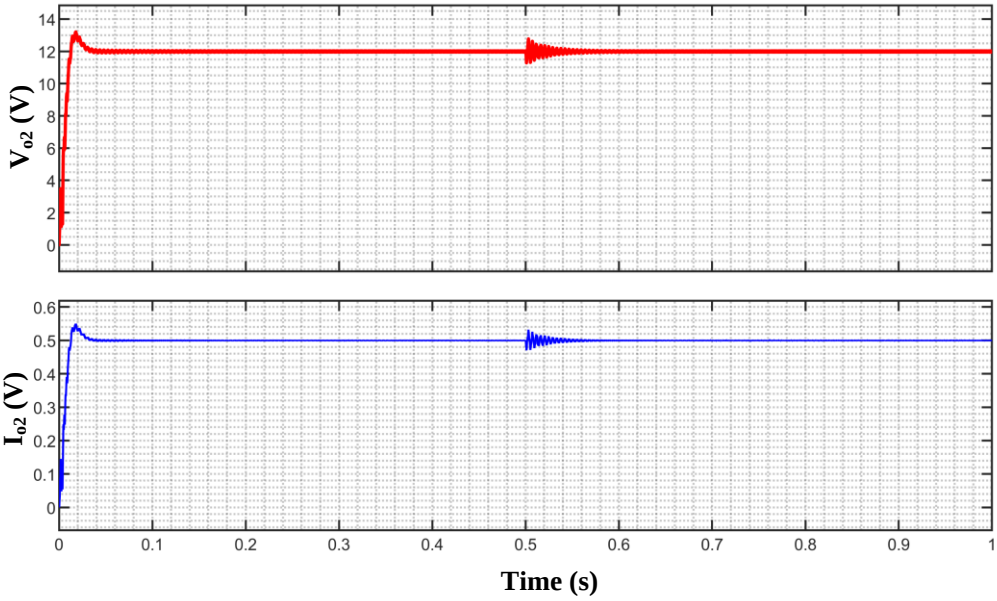

(b)

Fig 5.12 Load regulation effect when R1 changes from 96Ω to 72Ω on: (a) Boost Voltage (b) Buck Voltage

Now when the boost resistance was changed from 96 ohms to 48 ohms at 0.5 seconds, the output voltage showed quick stability with few oscillations, settling within 15 ms and displaying a minimal overshoot of just 0.9%. Under the same load variation, the buck converter stabilized somewhat later—about 19 ms—and experienced a far higher overshoot of 10%.

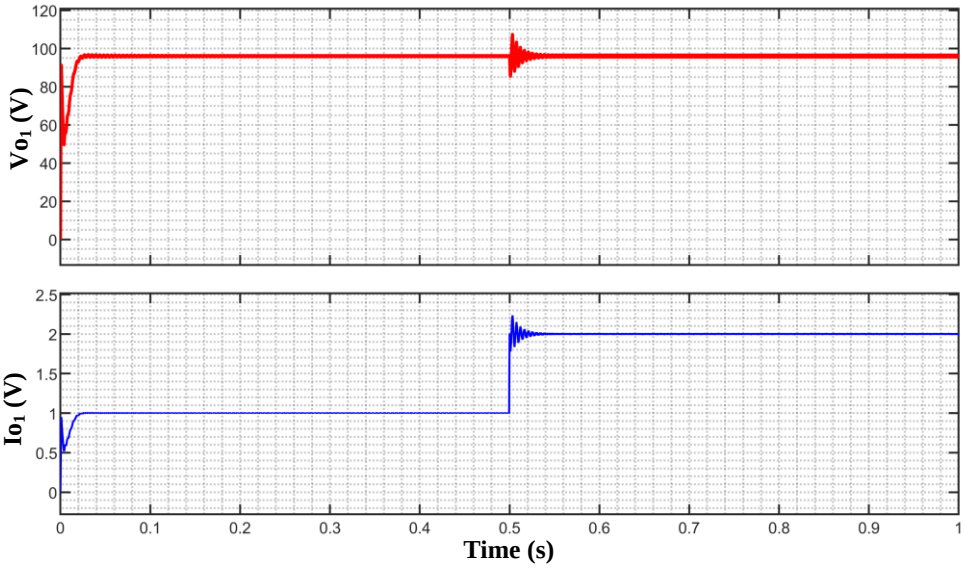

(a)

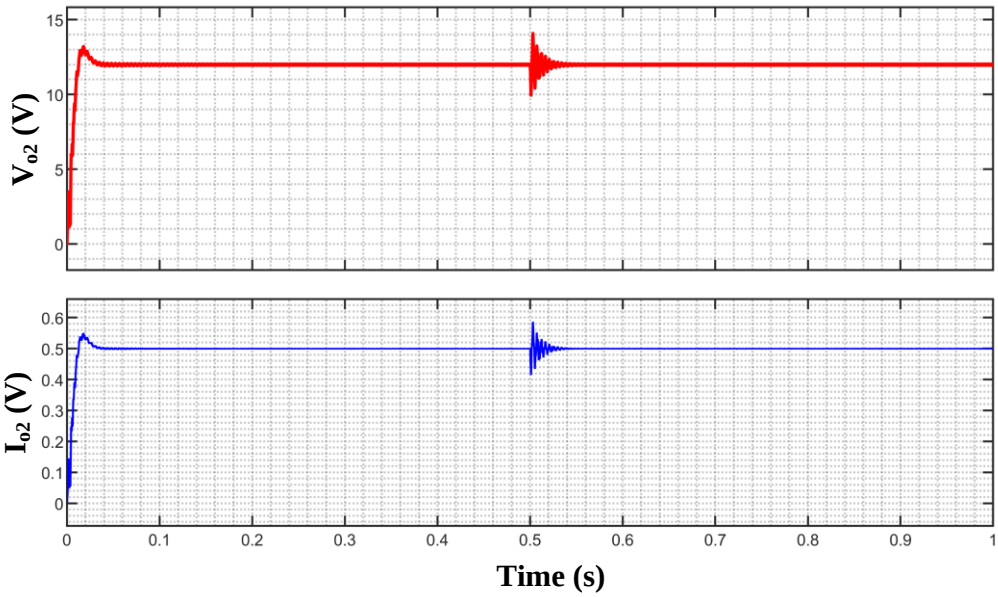

(b)

Fig 5.13 Load Regulation effect when R_1change 96Ω to 48Ω on: (a) Boost Voltage (b) Buck Voltage

Upon varying the buck resistance from 24 ohms to 18 ohms at 0.5 seconds within a single-input, double-output boost converter setup, remarkable load regulation was observed. The boost output voltage proved to be resilient, showing negligible impact and virtually no overshoot, indicative of exceptional load handling and stability. Simultaneously, the buck voltage adapted to the same resistance change, settling in 19 ms with an impressively low overshoot of just 0.6%. These findings underscore the converter's robust performance and highlight its potential for applications requiring precise voltage regulation under dynamic load conditions.

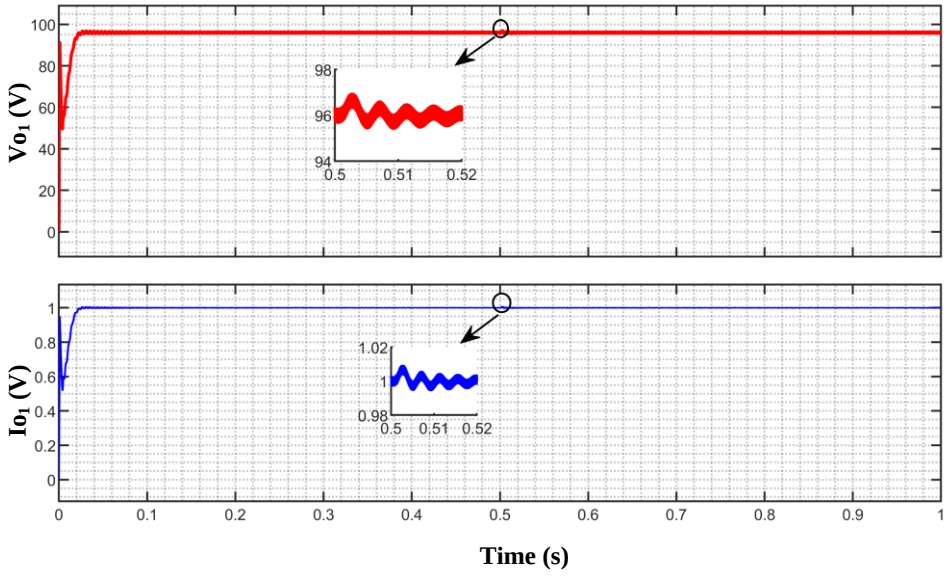

(a)

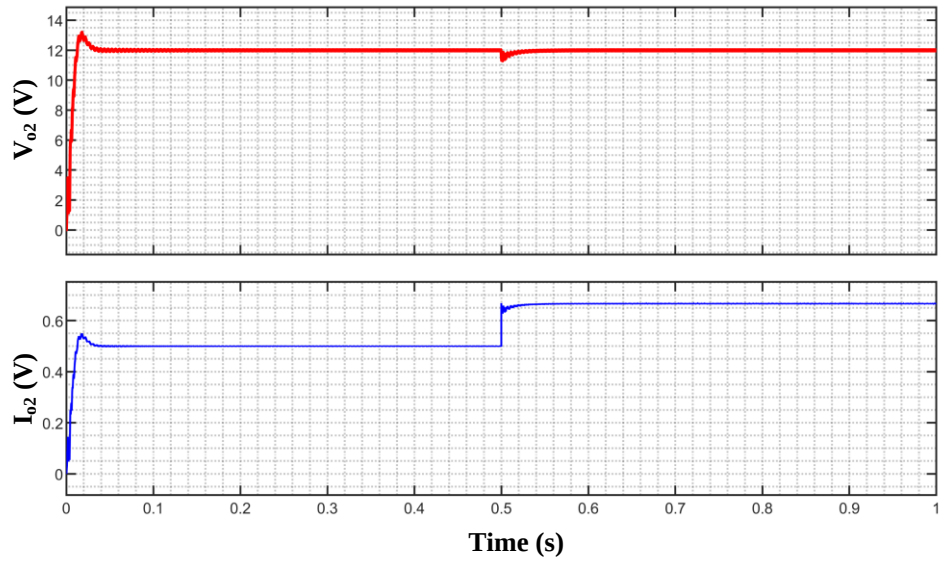

(b)

Fig 5.14 (b) Load Regulation effect when R_2 change 24Ω to18Ω on: (a) Boost Voltage (b) Buck Voltage

5.4.5 LINE REGULATION:

Line regulation in a DC-DC converter refers to the ability of the converter to maintain a stable output voltage despite variations in the input voltage. It is a critical performance metric that indicates how well the converter can reject fluctuations in the supply voltage and deliver a consistent output. Line regulation is typically expressed as a percentage and is defined as the change in output voltage as a function of the change in input voltage. In practical terms, good line regulation means that the output voltage remains nearly constant even when there are significant variations in the input

voltage. This stability is achieved through feedback control mechanisms that continuously adjust the operation of the converter, such as the duty cycle of the switching elements, to compensate for changes in the input voltage. Effective line regulation is essential for ensuring the reliable performance of electronic devices, particularly in environments where the input voltage can fluctuate due to variations in the power supply or other external factors. A DC-DC converter with good line regulation ensures that the load receives a consistent voltage, which is crucial for the proper functioning of sensitive electronic components and systems.

An investigation of the line regulation features of a boost converter with a single input and double outputs demonstrates its response to changes in input voltage. Despite a decrease in the input voltage from 48V to 45V, the converter's performance remained consistent. The boost output exhibited a minor oscillation, but quickly stabilized at a steady 96V within a mere 19 ms, with a modest deviation of 3% above the desired level. Simultaneously, the converter's buck output swiftly adjusted, reaching a stable voltage of 12V in just 15 ms, despite encountering a larger than expected overshoot of 10%. The difference in overshoot between the boost and buck outputs offers significant information about the converter's ability to regulate efficiently as the input conditions change.

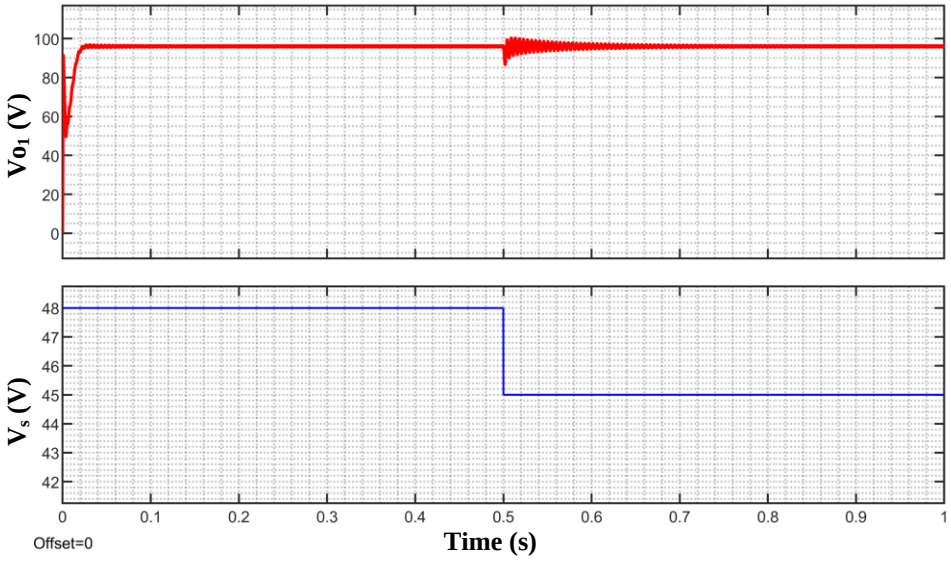

Fig 5.15 Line Regulation effect on boost output voltage when input voltage changes 48V to 45V

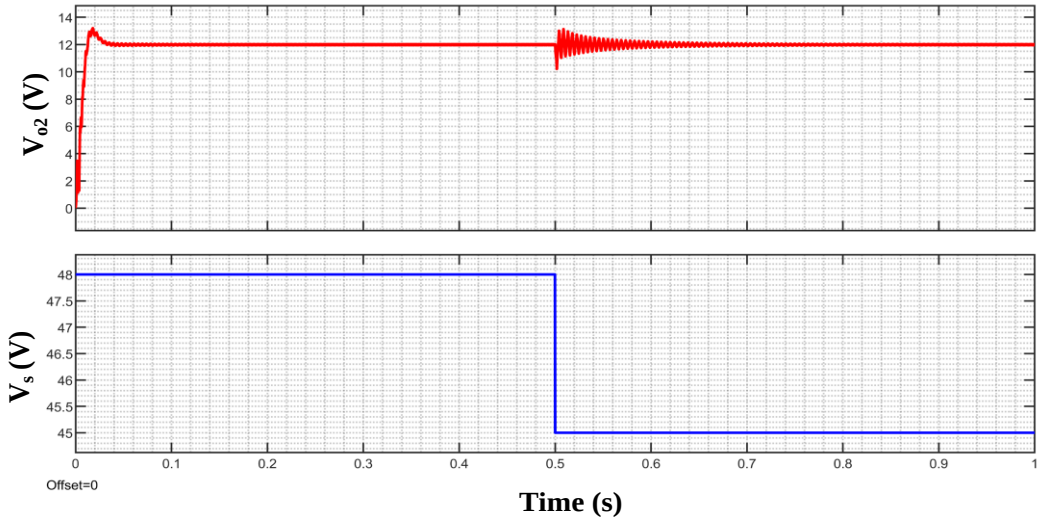

Fig 5.16 Line variation effect on buck output voltage when input voltage change 48V to 45V

Examining a single-input, double-output boost converter, special attention was paid to its line control features when input voltage from 48V to 55V changed. After this change, the boost output voltage showed only some ringing but remarkably achieved stability at 96V within 15 milliseconds, resulting in an overshoot of 9%. Though with an 8% overshoot, the buck output voltage showed endurance by correcting to a stable 12V in an accelerated 10 milliseconds at simultaneously. These results highlight the converter's dependability and efficiency in practical uses as they show how well it maintains output stability among different input voltages.

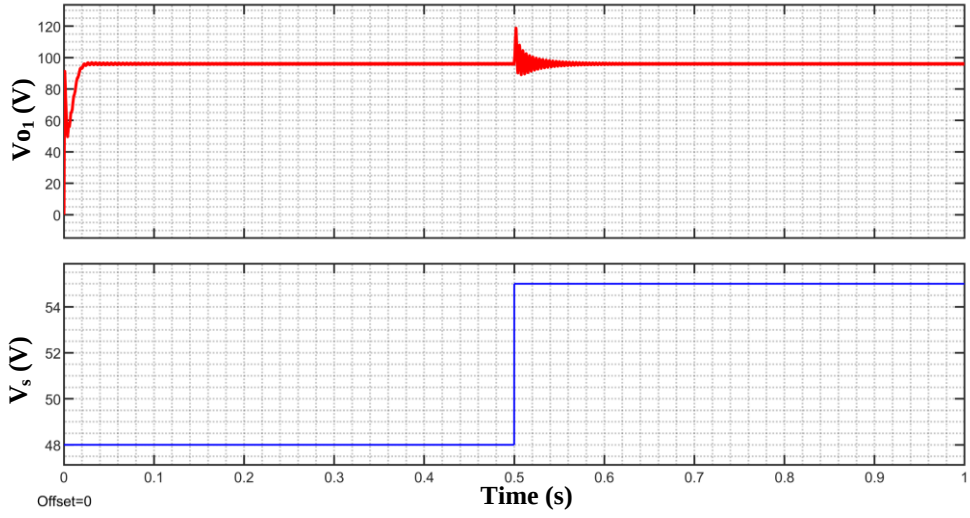

Fig 5.17 Line variation effect on boost output voltage when input voltage changes 48V to 55V

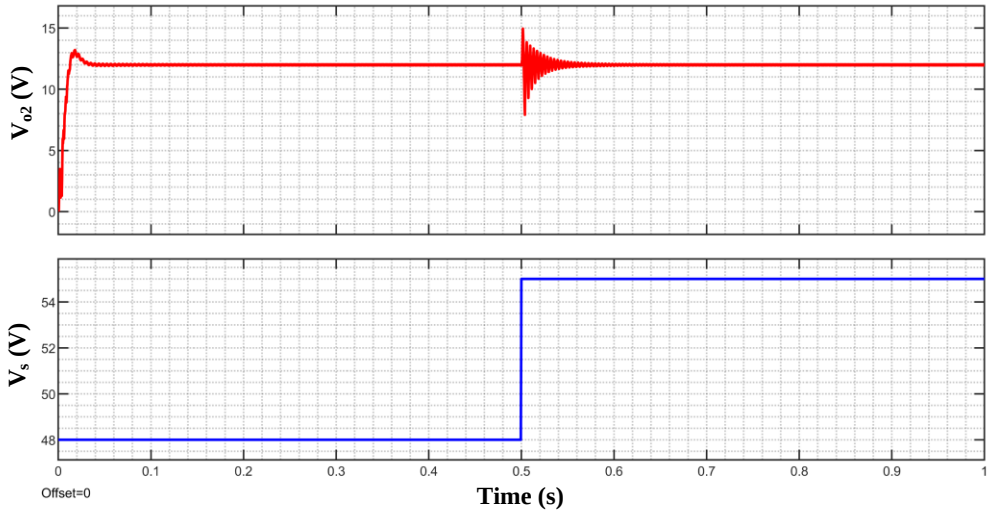

Fig 5.18 Line variation effect on buck output voltage when input voltage change 48V to 55V

5.3 CONCLUSIONS

This study demonstrated the efficacy of employing mathematical modelling and proportional integral (PI) control to enhance voltage regulation in Single Input Dual Output (SIDO) Step-Up and Step-Down converter. The closed loop control system's behavior has been confirmed in terms of both cross-regulation and voltage regulation of the converter. By utilizing these techniques, we have effectively addressed challenges arising from load variations and line fluctuations, ensuring consistent output voltages. The results indicate that the suggested converter exhibits excellent cross-regulation in response to both step load changes and dynamic reference changes in the output. Moreover, the implementation of PI control has enabled us to achieve significant improvements in voltage gain, contributing to the overall stability and performance of the converters. This research underscores the importance of advanced control strategies and modelling techniques in optimizing converter operation for diverse applications.

CHAPTER 6
CONCLUSIONS AND FUTURE SCOPE

6.1 CONCLUSIONS

1. Exploring closed-loop voltage mode control in half-bridge DC converters reveals substantial advantages in the field of power electronics. By conducting a thorough analysis using small-signal models, this study sheds light on the system's stability, responsiveness to transient steps, and bandwidth properties.

After a thorough analysis, the ideal input capacitor value was determined to be 200 µF. This choice is crucial for enhancing the system's stability, as demonstrated by a phase margin of 78 degrees that has been successfully attained. This choice demonstrates the system's ability to consistently maintain a 48V output even when there are sudden changes in the load.

2. Achieving reliable output under variable loads (from 26Ω to 48Ω) highlights the significance of precise control parameter selection. Ensuring optimal system performance in various operational conditions and application environments is of utmost importance. The control strategy's versatility, which can be adjusted to various power levels and specific application needs, enhances its usefulness. Nevertheless, the effectiveness of this approach relies heavily on the accurate adjustment of controller parameters. It is crucial to emphasize the importance of conducting additional research in order to fully grasp and improve this control strategy.

3. The analysis of the single-input, double-output boost converter highlights its capacity to dynamically regulate power in response to varying load and input conditions. The analysis emphasized the converter's adeptness in managing variances, hence guaranteeing stability and efficiency in power conversion. The system's ability to quickly adjust is shown in how both the boost and buck outputs respond to changes in load resistance. Particularly noteworthy is the system's capacity to maintain output stability with minimum overshoot, which serves as evidence of its well-designed and operationally reliable nature.

4. By analysing the system under various input voltage circumstances, we can gain a deeper understanding of the converter's resilience. The capacity to rapidly reach stabilization while maintaining manageable overrun percentages demonstrates its

durability and efficiency.

5. Analysed the reactions of boost and buck outputs to gain a comprehensive grasp of the system's adaptable performance in different scenarios. Both outputs exhibited effective stabilization and control over overshoots. However, slight differences in their responses highlight the intricate design factors that influence the converter's overall reliability and performance efficiency. The findings of this study have important ramifications for the progress of power electronics. The SIDO boost converter demonstrates its reliability by consistently delivering a stable output under various settings. This establishes a standard for regulatory efficiency, which is crucial for a wide range of applications that demand accurate voltage regulation.

6. The thorough examinations performed on both the half-bridge buck converter and the single-input, double-output boost converter provide valuable insights into the possibility of improving DC-DC converter designs for better efficiency, stability, and reaction in different situations. The identification of optimal settings, whether through the selection of components or the tuning of control parameters, is a common and critical aspect for both systems. This highlights the significance of precision in design and configuration in order to achieve higher performance.

6.2 FUTURE SCOPE OF STUDY

Expanding on the existing groundwork of this research, there are extensive and diverse opportunities for furthering the study of DC-DC converters. Various applications could greatly benefit from further study in crucial areas, which would expand the knowledge and effectiveness of these systems. The following items are included:

a. **Optimization of Controller Parameters:** Constant research on the optimization of controller parameters is much needed. This entails adjusting these settings to certain operational situations with different power levels and application needs. More resilient and flexible converter systems follow from much enhanced flexibility and efficiency of control techniques by means of better parameters.

b. **Comparative Analysis of Control Strategies:** Future research ought to also investigate several control approaches in comparison. This would entail looking for the most successful solutions by assessing several strategies under several operational

scenarios. These kinds of research not only help to clarify the relative merits and shortcomings of every approach but also direct the choice of certain uses so guaranteeing best performance.

c. **Investigating non-linear controllers**—such as sliding mode and model predictive controllers—would help the field much as it would assist you. In controlling the inherent non-linearities of converter systems, these kinds of controllers could provide exceptional performance. Research in this field could produce more strong and effective answers, therefore offering a significant advance in control technology.

d. **Integration of Smart Components:** Including smart components such as microcontrollers and sophisticated sensors will transform the operation of DC-DC converters. Integration of these technologies should be the main focus of next studies to allow adaptive changes and real-time system monitoring. This integration will greatly improve the operating efficiency and responsiveness of the system, therefore opening the path for more intelligent, flexible power electronic systems.

e. **Development of High-Frequency Converters:** High-frequency DC-DC converters have a strong case to be developed. Smaller component sizes and increased efficiency could come from research meant to challenge operating frequency limits. Applications where space and energy consumption are key issues depend especially on this. Investigating this path might produce innovations in small, high-performance converter designs.

By tackling these possible research avenues, future work can expand on the present knowledge base, filling inefficiencies and creating fresh directions in the design and application of DC-DC converters. These initiatives will not only improve theoretical knowledge but also propel pragmatic technological developments in line with changing requirements for power electronics uses.

2 LIST OF PUBLICATIONS

1. K. Gaurav, D. Joshi and S. Upadhyaya, "Advancing Voltage Stability in Half-Bridge Isolated DC-DC Converter through the Adoption of PI Controller," *2023 11th National Power Electronics Conference (NPEC)*, Guwahati, India, 2023, pp. 1-5, doi: 10.1109/NPEC57805.2023.10384896.
2. K. Gaurav, D. Joshi Ashutosh and S. Upadhyaya, "Enhanced Gain Double - Output Boost/Buck DC-DC Converter," 15th *International IEEE Conference on Computing, Communication and Networking Technologies* (ICCCNT) (Accepted)

3 REFERENCES

[1] Xinyu Xu, A. M. Khambadkone and R. Oruganti, "An asymmetrical half bridge DC-DC converter: close loop design in frequency domain," 2004 IEEE 35th Annual Power Electronics Specialists Conference (IEEE Cat. No.04CH37551), Aachen, Germany, 2004, pp. 1642-1647 Vol.2, doi: 10.1109/PESC.2004.1355672.

[2] B. Choi, W. Lim, Sanghyun Bang and Seungwon Choi, "Small-signal analysis and control design of asymmetrical half-bridge DC-DC converters," in IEEE Transactions on Industrial Electronics, vol. 53, no. 2, pp. 511-520, April 2006, doi: 10.1109/TIE.2006.870715.

[3] A. J. Perin and I. Barbi, "A new isolated half-bridge soft-switching pulse-width modulated DC-DC converter," [Proceedings] APEC '92 Seventh Annual Applied Power Electronics Conference and Exposition, Boston, MA, USA, 1992, pp. 66-72, doi: 10.1109/APEC.1992.228429.

[4] W. Eberle and Yan-Fei Liu, "A zero voltage switching asymmetrical half-bridge DC/DC converter with unbalanced secondary windings for improved bandwidth," 2002 IEEE 33rd Annual IEEE Power Electronics Specialists Conference. Proceedings (Cat. No.02CH37289), Cairns, QLD, Australia, 2002, pp. 1829-1834 vol.4, doi: 10.1109/PSEC.2002.1023076.

[5] F. F. Linera, J. Sebastian, M. A. Perez Garcia, J. Diaz and A. Fontan, "Closing the feedback loop in the half-bridge complementary-control DC-to-DC converter," Proceedings of APEC 97 - Applied Power Electronics Conference, Atlanta, GA, USA, 1997, pp. 977-982 vol.2, doi: 10.1109/APEC.1997.575766.

[6] T. Ninomiya, N. Matsumoto, M. Nakahara and K. Harada, "Static and dynamic analysis of zero-voltage-switched half-bridge converter with PWM control," PESC '91 Record 22nd Annual IEEE Power Electronics Specialists Conference, Cambridge, MA, USA, 1991, pp. 230-237, doi: 10.1109/PESC.1991.162681.

[7] Erickson, R. W., Maksimovic, D. (2001). Fundamentals of Power Electronics. Springer.

[8] D.W. Hart, "Power Electronics," McGraw-Hill, New York, NY, USA, 2011.

[9] O. Tahmaz and A. B. Yıldız, "Efficient Modeling Technique for Analysis of the

Half Bridge DC-DC Converter," 2021 23rd European Conference on Power Electronics and Applications (EPE'21 ECCE Europe), Ghent, Belgium, 2021, pp. P.1-P.10, doi: 10.23919/EPE21ECCEEurope50061.2021.9570626.

[10] Hong Mao, Songquan Deng, Yangyang wen and Issa Batarseh, "Unified steady-state model and DC analysis of half-bridge DC-DC converters with current doubler rectifier," Nineteenth Annual IEEE Applied Power Electronics Conference and Exposition, 2004. APEC '04., Anaheim, CA, USA, 2004, pp. 786-791 vol.2, doi: 10.1109/APEC.2004.1295912.

[11] Xinyu Xu, A. M. Khambadkone and R. Oruganti, "Analysis and design of an optimized asymmetrical half-bridge DC-DC converter," The Fifth International Conference on Power Electronics and Drive Systems, 2003. PEDS 2003., Singapore, 2003, pp. 120-125 Vol.1, doi: 10.1109/PEDS.2003.1282697.

[12] P. Imbertson and N. Mohan, "Asymmetrical duty cycle permits zero switching loss in PWM circuits with no conduction loss penalty," in IEEE Transactions on Industry Applications, vol. 29, no. 1, pp. 121-125, Jan.-Feb. 1993, doi: 10.1109/28.195897.

[13] O. Ray, A. P. Josyula, S. Mishra and A. Joshi, "Integrated Dual-Output Converter," in IEEE Transactions on Industrial Electronics, vol. 62, no. 1, pp. 371-382, Jan. 2015, doi: 10.1109/TIE.2014.2327599.

[14] P. Shamsi and B. Fahimi, “Dynamic behavior of multiport power electronic interface under source/load disturbances,” IEEE Trans. Ind. Electron., vol. 60, no. 10, pp. 4500–4511, Oct. 2013.

[15] C. N. Onwuchekwa and A. Kwasinski, “A modified-time-sharing switching technique for multiple-input DC–DC converters,” IEEE Trans. Power Electron., vol. 27, no. 11, pp. 4492–4502, Nov. 2012.

[16] R. Adda, O. Ray, S. Mishra, and A. Joshi, “Synchronous reference frame-based control of switched boost inverter for standalone DC nanogrid applications,” IEEE Trans. Power Electron., vol. 28, no. 3, pp. 1219–1233, Mar. 2013.

[17] A. V. Stankovic, L. Nerone, and P. Kulkarni, “Modified synchronous buck converter for a dimmable HID electronics ballast,” IEEE Trans. Ind.Electron., vol. 59, no. 4, pp. 1815–1824, Apr. 2012.

[18] H. Chen, Y. Zhang, and D. Ma, “A SIMO parallel-string driver IC for

dimmable LED backlighting with local bus voltage optimization and single time-shared regulation loop," IEEE Trans. Power Electron., vol. 27,no. 1, pp. 452–462, Jan. 2012.

[19] J.-K. Kim, S.-W. Choi, C.-E. Kim, and G.-W. Moon, "A new standby structure using multi-output full-bridge converter integrating flyback converter," IEEE Trans. Ind. Electron., vol. 58, no. 10, pp. 4763–4767,Oct. 2011.

[20] Linear Technology, LTC 2-Cell, Multi-Output DC/DC Converter with USB Power Manager, Milpitas, CA, USA. [Online]. Available: http://www.linear.com/product/LTC3456

[21] M. Rodriguez, G. Stahl, L. Corradini, and D. Maksimovic, "Smart DC power management system based on software-configurable power modules," IEEE Trans. Power Electron., vol. 28, no. 4, pp. 1571–1586,Apr. 2013.

[22] A. Emadi and M. Ehsani, "Multi-converter power electronic systems: Definition and applications," in Proc. IEEE PESC, 2001,vol. 2, pp. 1230–1236.

[23] X. Wu, L. Tian, and Y. Liang, "Single inductor, multiple output dc-dc converter," May 25 2017, uS Patent App. 15/256,575.

[24] J. Chen, V. Mayega, D. W. Evans, and J. L. Krug, "Single inductor dual output buck converter," May 29 2007, uS Patent 7,224,085.

[25] [C.-S. Huang, D. Chen, and K. H. Liu, "Mix-voltage conversion for single-inductor dual-output buck converters," in Energy Conversion Congress and Exposition, 2009. ECCE 2009. IEEE. IEEE, 2009, pp.639–646.

[26] D. Kwon and G. A. Rincon-Mora, "Single-inductor–multiple-output

[27] switching dc–dc converters," IEEE Transactions on Systems II: Express Briefs, vol. 56, no. 8, pp. 614–618, 2009.

[28] J.-M. Chang and M. Pedram, "Energy minimization using multiple supply voltages," IEEE Transactions on Very Large-Scale Integration (VLSI) Systems, vol. 5, no. 4, pp. 436–443, 1997.

[29] T. Ishihara and K. Asada, "A system level memory power optimization technique using multiple supply and threshold voltages," in Proceedings of the 2001 Asia and South Pacific Design Automation Conference. ACM, 2001, pp. 456–461.

[30] Rong-Jong Wai, Kun-Huai Jheng, "High-Efficiency Single Input Multiple Output

DC-DC Converter," IEEE Transactions on Power Electronics, Vol.28, No.2, February 2013.

[31] [2] P. Patra, A. Patra, and N. Misra, "A single-inductor multiple-output switcher with simultaneous buck, boost, and inverted outputs," IEEE Transactions on Power Electron, vol. 27, no. 4, pp. 1936–1951, Apr.2012.

[32] [3] A. Nami, F. Zare, A. Ghosh, and F. Blaabjerg, "Multiple-output DC–DC converters based on diode-clamped converters configuration: Topology and control strategy," IET Power Electronics, vol. 3, no. 2, pp. 197–208,2010.

[33] Kumar, J. Sai, and Tikeshwar Gajpal. "A Multi Input DC-DC Converter for Renewable Energy Applications." (2016).

[34] [2] Ortiz, G., J. Biela, D. Bortis, and J. W. Kolar. "1 Megawatt, 20 kHz, isolated, bidirectional 12kV to 1.2 kV DC-DC converter for renewable energy applications." In Power Electronics Conference (IPEC), 2010 International, pp. 3212-3219. IEEE, 2010.

[35] [3] Li, Wuhua, Xiaodong Lv, Yan Deng, Jun Liu, and Xiangning He. "A review of non-isolated high step-up DC/DC converters in renewable energy applications." In Applied Power Electronics Conference and Exposition, 2009. APEC 2009. Twenty-Fourth Annual IEEE, pp. 364-369. IEEE, 2009.

[36] Y. Chen, Y. Kang, S. Nie, and X. Pei, "The multiple-output DC–DC converter with shared ZCS lagging leg," IEEE Transactions on Power Electronics,vol. 26, no. 8, pp. 2278–2294, Aug. 2011.

[37] [5] Maria Bella Ferrera Prieto, Salvador Perez Litran, Eladio Duran Aranda, Juan Manuel Enrique Gomez,"New Single- Input, Multiple-Output Converter Topologies," IEEE Industrial Electronics Magazine, Vol. 10, no 2, pp. 6 – 20,2016.

[38] [6] R. J.Wai and R. Y. Duan, "High step-up converter with coupled inductor," IEEE Transactions Power Electronics, vol. 20, no. 5, pp. 1025–1035, Sep. 2005.

PAPER NAME

Gaurav_thesis.pdf

WORD COUNT

13090 Words

CHARACTER COUNT

69370 Characters

PAGE COUNT

56 Pages

FILE SIZE

5.4MB

SUBMISSION DATE

May 30, 2024 9:39 PM GMT+5:30

REPORT DATE

May 30, 2024 9:40 PM GMT+5:30

10% Overall Similarity

The combined total of all matches, including overlapping sources, for each database.

- 2% Internet database
- 6% Publications database
- Crossref database
- Crossref Posted Content database
- 7% Submitted Works database

Excluded from Similarity Report

- Bibliographic material
- Cited material
- Small Matches (Less then 10 words)
- Manually excluded sources